Available online at www.sciencedirect.com
SCIENCE DIRECT®
Geochimica et Cosmochimica Acta 70 (2006) 1077–1096
Geochimica
www.elsevier.com/locate/gca

Isotopic effects in fracture-dominated reactive fluid–rock systems

Donald J. DePaolo *

Earth Sciences Division, E.O. Lawrence Berkeley National Laboratory and Department of Earth and Planetary Science, University of California, Berkeley, CA 94720, USA

Received 22 July 2005; accepted in revised form 9 November 2005

Abstract

A mathematical model is presented that describes the effects of pore fluid aqueous diffusion and reaction rate on the isotopic exchange between fluids and rocks in reactive geo-hydrological systems where flow is primarily through fractures. The model describes a simple system with parallel equidistant fractures, and chemical transport in the matrix slabs between fractures by aqueous diffusion through a stagnant pore fluid. The solid matrix exchanges isotopes with pore fluid by solution–precipitation at a rate characterized by a time constant, R (yr^{-1}), which is an adjustable parameter. The effects of reaction on the isotopes of a particular element in the fracture fluid are shown to depend on the ratio of the diffusive reaction length for that element (L) to the fracture spacing (b). The reaction length depends on the solid–fluid exchange rate within the matrix, the partitioning of the element between the matrix pore fluid and the matrix solid phase, the porosity and density of the matrix, and the aqueous diffusivity. For $L/b < 0.3$, fluid–rock isotopic exchange is effectively reduced by a factor of $2L/b$ relative to a standard porous flow (single porosity) model. For $L/b > 1$, the parallel fracture model is no different from a porous flow model. If isotopic data are available for two or more elements with different L values, it may be possible to use the model with appropriate isotopic measurements to estimate the spacing of the primary fluid-carrying fractures in natural fluid–rock systems. Examples are given using Sr and O isotopic data from mid-ocean ridge (MOR) hydrothermal vent fluids and Sr isotopes in groundwater aquifers hosted by fractured basalt. The available data for MOR systems are consistent with average fracture spacing of 1–4 m. The groundwater data suggest larger effective fracture spacing, in the range 50–500 m. In general, for fractured rock systems, the effects of fracture–matrix diffusive exchange must be considered when comparing isotopic exchange effects for different elements, as well as for estimating water age using radioactive and cosmogenic isotopes.

1. Introduction

The isotopic compositions of fluids in natural fluid–rock systems are useful for characterizing flow paths, transport rates by diffusion and advection, and the rates of fluid–rock chemical exchange. Examples of the use of both light stable isotopes and radiogenic isotopes for these purposes are abundant in the recent literature (Lasaga, 1984; Bickle and McKenzie, 1987; Richter and DePaolo, 1987, 1988; Lassey and Blattner, 1988; Blattner and Lassey, 1989; Bickle and Chapman, 1990; Bickle, 1992; Bickle and Teagle, 1992; Schrag et al., 1992; Lasaga and Rye, 1993; Johnson and DePaolo, 1994; Schrag et al., 1995; DePaolo and Getty, 1996; Skelton et al., 1997; Baxter and DePaolo, 2000; Johnson et al., 2000). The standard approach treats fluid–rock systems as equivalent porous media, which might also be called "single porosity" (sp) systems (Bear, 1979). However, fluid flow in many natural systems is not evenly distributed through the rock pore space, but instead is localized along fractures or high-permeability zones (e.g., Evans and Nicholson, 1987; Bear, 1992). Isotopic effects in fractured rock systems are likely to be different from those in the simpler models, largely due to the difference in geochemical transport modes between the fluids flowing in the fractures and the fluids trapped in the rock material separating the fractures. These effects have been explored in some detail for radiocarbon and tritium ages of groundwater (Tang et al., 1981; Sudicky and Frind, 1982; Maloszewski and Zuber, 1991; Sanford, 1997).

* Fax: +1 510 642 9520.
E-mail address: depaolo@eps.berkeley.edu.

0016-7037/$ - see front matter © 2005 Elsevier Inc. All rights reserved.
doi:10.1016/j.gca.2005.11.022

This paper presents a relatively simple analytical model that describes the isotopic shifts of commonly measured elements with natural isotopic variations (e.g., Sr, O, U) in fluids moving through and reacting with fractured porous rock. The objective is to better understand fluid and rock isotopic evolution in the so-called "dual porosity" or "dual permeability" (dp) fluid–rock systems, and to evaluate the relationships between isotopic effects, fluid–rock reaction rates, and fracture spacing (see Table 1).

The simplest model of a dp system is one in which water flows in parallel fractures, which are separated by slabs of porous rock "matrix" containing stagnant pore fluid (Fig. 1; cf. Sudicky and Frind, 1982; Sanford, 1997). The fluid moving through the fractures interacts thermally and chemically with the matrix between the fractures by the conduction of heat and the diffusion of chemical constituents dissolved in the pore fluid or vapor phase. The extent to which water–rock exchange in the matrix blocks affects the chemical and isotopic composition of the fracture fluid depends on the rate of migration of chemical species from the matrix block interiors to the surfaces of the fractures. Different chemical elements can be affected to differing degrees, depending on their solubility and diffusion coefficient in the fluid phase, and the solid–fluid exchange rate in the matrix slabs. Because of the diffusion effects in the matrix pore fluid, isotopic ratios of certain pairs of elements can, in theory, be used to assess the average fracture spacing in a dp system—information that is generally difficult to obtain. In natural systems, the spacing of fractures can be estimated from rock outcrops and drill core observations, but the spacing of the fractures actually carrying the bulk of the fluid is usually not known directly.

Previous work on matrix diffusion has treated the effects on retardation of chemical and isotopic species (e.g., Tang et al., 1981; Sudicky and Frind, 1982; Wilson and Dudley, 1987; Neretneiks, 1992), the nature of reaction fronts (Steefel and Lichtner, 1998a,b), or the effect on radiocarbon and tritium ages (Maloszewski and Zuber, 1991; Sanford, 1997). The papers dealing with contaminant transport deal mainly with ion exchange reactions and assume the ion exchange reactions to take place instantaneously. Sanford (1997) models mainly the aqueous diffusion of carbon species be-

Table 1
Summary of notation

Symbol	Definition	Units
b	Spacing between fractures	L
d	Width of fracture	L
L	Reaction length for diffusive pore fluid transport	L
L_a	Reaction length for advection	L
L_{sp}	Reaction length for diffusion, with reaction rate = R_{sp}	L
L_r	Decay length	L
ϕ	Porosity	None
ϕ_m	Matrix porosity	None
ϕ_f	Porosity within the fracture	None
ρ_s, ρ_f	Density of solid, fluid	M/L^3
C_f, C_s, C_p	Concentration in fluid (f), solid (s), matrix pore fluid (p)	mol/L^3
R	Bulk reaction time constant	T^{-1}
R_{di}	Dissolution time constant for phase i	T^{-1}
R_{pj}	Precipitation time constant for phase j	T^{-1}
R_m	Bulk reaction time constant for solid in the matrix of a fractured system	T^{-1}
K	Distribution coefficient for solid/fluid (element or major isotope)	None
K^*	Distribution coefficient for second isotope	None
D, D_i	Aqueous diffusivity, subscript to denote specific element	L^2/T
D_v	Dispersion coefficient	L^2/T
D_C	Aqueous diffusivity for dissolved carbon species	L^2/T
v	Fluid velocity for porous flow	L/T
v_f	Velocity of fluid in a fracture	L/T
M	Mass ratio of solid/fluid	None
C^*	Concentration of a radiogenic isotope (e.g., ^{87}Sr) or minor heavy isotope (^{18}O)	mol/L^3
α	Equilibrium isotopic fractionation factor	None
Δ	$1000 \ln \alpha$	None
r_s, r_f, r_p	Isotopic ratio in solid (s), fluid or fracture fluid (f), matrix pore fluid (p)	None
τ_s	Timescale for isotopic adjustment of the solid phase	T
τ_f	Timescale for isotopic adjustment of the fluid phase	T
τ_a	Advection timescale	T
τ_i	Time for matrix pore fluid to reach isotopic steady state for element i	T
q	Fluid flux	L/T
δ_s, δ_f	Delta value of solid, fluid (e.g., $\delta^{18}O$)	None
A_n	Fourier series coefficient	None
λ_n	Decay constant for Fourier series coefficients	T^{-1}
t_u	Uncorrected or observed radiocarbon age of groundwater	T
t_c	Corrected radiocarbon age of groundwater	T
t_R	Total reaction time for fluid in a groundwater or hydrothermal system	T

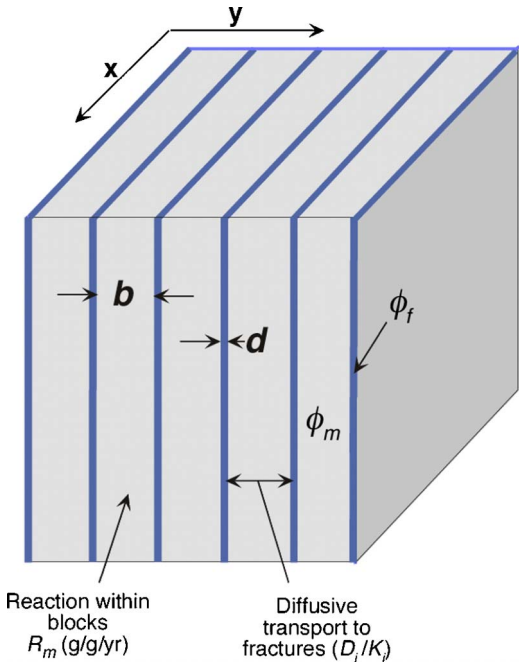

Fig. 1. Conceptual model of the dual porosity medium. Fluid in fractures with width d and porosity ϕ_f moves in the x-direction at velocity v_f. Fracture spacing is b, and matrix porosity is ϕ_m. The solid within the matrix reacts with the fluid by solution and reprecipitation at a rate of R_m g g^{-1}yr^{-1}. Chemical transport within the matrix in the y-direction is controlled by the porosity and the elemental diffusivity in the fluid (D_i), and by the partitioning of the element between the solid and fluid phase (K_i is the ratio of concentration in the solid phase to the concentration in the fluid phase).

tween stagnant ^{14}C-depleted matrix pore fluid and fracture fluids containing ^{14}C. Maloszewski and Zuber (1991) develop a model for radiocarbon ages in waters in carbonate aquifers analogous to that presented here in that it accounts for carbon exchange reactions between fluids and solids.

In this paper, the reactions are assumed to be heterogeneous, and the rate of reaction (i.e., the rate of solid–fluid exchange; mainly by solution–precipitation reactions) is a free parameter, the value of which is a strong determinant of the behavior of the system. The fracture spacing is also allowed to be finite, and either relatively small or large in comparison to diffusion distances in the matrix pore fluid. Bickle (1992) and Bickle and Teagle (1992) discuss the role of matrix diffusion in a context similar to that addressed here, but their treatment of fracture flow systems does not allow for variations in the reaction rate in the matrix. Skelton et al. (1997) discuss the possibility that kinetic dispersion in a metamorphic system is related to fracture spacing and use an approximate formulation from Bickle (1992) to estimate fracture spacing.

2. Model equations

2.1. Porous flow reference model

The standard porous flow model for isotopic exchange is covered in many publications and textbooks, but a few key equations are presented here, using notation that is consistent with that used for the fracture flow model described in the next section. The porous flow model serves as a reference case with which the fracture model can be compared.

The equation, in one dimension, that can be used to describe the evolution of the concentration of a dissolved trace constituent in fluid flowing through and reacting with a porous rock matrix is (e.g., Navon and Stolper, 1987; Lassey and Blattner, 1988; Richter and DePaolo, 1988; Johnson and DePaolo, 1994; and many others)

$$\rho_f \frac{\partial \phi C_f}{\partial t} = \rho_f D \frac{\partial}{\partial x}\left(\frac{\partial \phi C_f}{\partial x}\right) - v\rho_f \frac{\partial \phi C_f}{\partial x} + \sum_i R_{di} C_{si} - \sum_j R_{pj} K_j C_f, \quad (1a)$$

where C_f is concentration (moles/gram) in the fluid (a function of x and t), D_v is dispersion coefficient in the fluid (including ionic diffusion) is a function of v, R_{di} is dissolution rate (grams of solid phase i dissolved/unit volume/time), R_{pj} is precipitation rate (grams of solid phase j precipitated/unit volume/time), C_{si} is concentration (moles/gram) in dissolving solid phase i, K_j is equilibrium distribution coefficient for precipitating phase j, v is fluid velocity, ϕ is porosity, ρ_f is density of the fluid.

When solids dissolve, they contribute stoichiometrically the trace element in question to the fluid phase dissolved load, and when solids precipitate from solution, they incorporate the trace element according to a distribution coefficient "K." In this formulation, because trace constituents are considered, the reaction rates R_{pj} and R_{di}, are independent of the concentrations. The reactions rates are often modeled as being dependent on the departure from major element equilibrium (e.g., Steefel and Lichtner, 1998a), but here the specific dependence of R_{pj} and R_{di} is of less concern, at least to describe the gross behavior of isotope ratio variations in simple systems. In many natural systems, it can be shown that the reaction rates do not conform to the standard kinetic theory formulation in any case (e.g., Maher et al., 2004, 2006).

The solid matrix does not move, so the evolution of the solid phase includes no transport terms; the equation simply describes how the solid at any place in the system changes in response to material exchange with the fluid that is present locally

$$(1-\phi)\rho_s \frac{\partial C_s}{\partial t} = -\sum_i R_{di}(C_{si} - C_s) + \sum_j R_{pj}(K_j C_f - C_s), \quad (1b)$$

Eqs. (1a) and (1b) require that fluid and solid density be constant in space and time; other parameters in the model can in general be considered to be functions of both space and time.

The simplest situation is provided by a monomineralic rock, and where the mineral dissolves and reprecipitates at a specified rate $R_p = R_d$, such that there is no change

in porosity (Richter and DePaolo, 1987). The equations then simplify to:

$$\frac{\partial C_f}{\partial t} = D_v \frac{\partial^2 C_f}{\partial x^2} - v\frac{\partial C_f}{\partial x} + RM(C_s - KC_f), \tag{2a}$$

where R in this case is the "bulk recrystallization time constant" with units of reciprocal time, and M is the mass ratio of solid to fluid

$$M = \frac{\rho_s(1-\phi)}{\rho_f \phi}.$$

The solid phase is then described by:

$$\frac{\partial C_s}{\partial t} = -R(C_s - KC_f). \tag{2b}$$

The fluid phase concentration responds to the dissolution and precipitation of all of the minerals in the rock. Hence for a multi-mineral solid, the simplified equation above can serve to provide a realistic description of the system as long as changes in porosity are minor. The bulk recrystallization time constant (R) in this case can be defined by:

$$\rho_s R = \sum_i f_i R_{di} + \sum_j f_j R_{dj}, \tag{2c}$$

where f_i is the volume fraction of primary minerals i in the solid phase, and f_j is the volume fraction of secondary minerals.

For most of the discussion here, analogues of Eqs. (2a) and (2b) will be used. The primary objective is to illustrate the effects of fracture flow on a simple system. This is justified insofar as the fluid composition reflects the (concentration-weighted) "bulk" dissolution of the solid. Extending the model to rocks with multiple minerals, especially where the dissolution rates vary greatly between minerals, is straightforward and instructive. Criss et al. (1987) and Gregory et al. (1989), for example, use oxygen isotopic data from pairs of minerals to understand rates of fluid evolution and timescales of fluid–rock exchange.

Eqs. (2a) and (2b) can be converted to an expression in terms of isotopic ratios, recognizing that an isotopic ratio is just the ratio of two concentrations (e.g., $r = C^*/C$):

$$C\mathrm{d}r = \mathrm{d}C^* - r\,\mathrm{d}C. \tag{3}$$

The complete equations for isotopic ratios (using similar notation) are given in Johnson and DePaolo (1994, 1997a). For the purposes of the model to be presented here, these will be simplified further from Eqs. (2a) and (2b) by ignoring the effects of dispersion. This yields for the evolution of the isotope ratio with time:

$$\frac{\mathrm{d}r_f}{\mathrm{d}t} = -v\frac{\mathrm{d}r_f}{\mathrm{d}x} + RM\frac{C_s}{C_f}[r_s - r_f] + RMK[r_f - \alpha r_f], \tag{4a}$$

$$\frac{\mathrm{d}r_s}{\mathrm{d}t} = -RK\frac{C_f}{C_s}[r_s - \alpha r_f], \tag{4b}$$

where $\alpha = K^*/K$ is the equilibrium isotopic fractionation factor between the bulk solid and the fluid. For isotope ratios that involve mass dependent fractionation (O, H, C, S, N, etc.) the parameter α is dependent on the mineralogy of the solid, the composition of the fluid, and temperature. For elements where the isotopic effects are generated by radioactive decay or other nuclear processes, it is appropriately assumed that $\alpha = 1$, in which case the third term on the right-hand side of Eq. (4a) vanishes. For an element like oxygen, $\alpha \neq 1$, but since in almost all cases it can be assumed that $K = C_s/C_f$, the equations reduce to:

$$\frac{\mathrm{d}r_f}{\mathrm{d}t} = -v\frac{\mathrm{d}r_f}{\mathrm{d}x} + RMK[r_s - \alpha r_f], \tag{4c}$$

$$\frac{\mathrm{d}r_s}{\mathrm{d}t} = -R[r_s - \alpha r_f]. \tag{4d}$$

Eqs. (4c) and (4d) are coupled and can be solved for specific initial and boundary conditions. When $MK \gg 1$ (and $MC_s/C_f \gg 1$), the system has two very different timescales, which allows for further simplifications. The effect of reactions between the solid and fluid is to cause both the fluid and the solid to approach the (isotopic) equilibrium condition, which is $r_s(x) = \alpha r_f(x)$. However, the rate of change of the fluid isotope ratio can differ greatly from the rate of change of the solid isotope ratio as a result of the mass balance term MC_s/C_f (this has been referred to in some cases as water/rock ratio, but that terminology is not used here because water/rock also has other connotations). The fluid approaches the equilibrium condition with a timescale of $\tau_f = (RMK)^{-1}$ (Eq. (4c)). The solid approaches the equilibrium condition with a timescale of $\tau_s = R^{-1}$. The ratio of these two timescales is $\tau_s/\tau_f = MK$.

For fluid–rock systems, the porosity is usually in the range 0.001–0.1, so M takes on values of about 25–2500. For many trace elements that have isotopic variations of interest, such as Sr, Pb, Nd, and U, the value of K is in the range 10–1000, and hence MK takes on values between 250 and 2.5×10^6. For these elements, interaction between the fluid and solid causes the isotopic composition of the fluid to change rapidly in comparison to the solid (Johnson and DePaolo, 1994; DePaolo and Getty, 1996). The implication of this can be appreciated by considering the steady state version of Eqs. (4a)–(4d), with the dimensions removed. The non-dimensionalization is done by defining a dimensionless time $t' = tv/\ell$ and a dimensionless distance $x' = x/\ell$. The lengthscale ℓ can be considered to be the length of the fluid path in the system, and hence the characteristic timescale is the fluid transit time $\tau_a = \ell/v$. The dimensionless forms of Eqs. (4a) and (4b) are then:

$$\frac{\mathrm{d}r_f}{\mathrm{d}t'} = -\frac{\mathrm{d}r_f}{\mathrm{d}x'} + \frac{RMK\ell}{v}[r_s - \alpha r_f], \tag{5a}$$

$$\frac{\mathrm{d}r_s}{\mathrm{d}t'} = -\frac{R\ell}{v}[r_s - \alpha r_f]. \tag{5b}$$

In terms of timescales, these equations can also be written in the following forms:

$$\frac{\mathrm{d}r_f}{\mathrm{d}t'} = -\frac{\mathrm{d}r_f}{\mathrm{d}x'} + \frac{\tau_a}{\tau_f}[r_s - \alpha r_f], \tag{6a}$$

$$\frac{dr_s}{dt'} = -\frac{1}{MK}\frac{\tau_a}{\tau_f}[r_s - \alpha r_f]. \quad (6b)$$

In many cases, the reaction rates are slow enough that the ratio $\tau_a/\tau_f \leqslant 1$, and during transit of the system the fluid makes only a fractional approach to isotopic equilibrium. If MK is large, this means that the solid will experience a negligible change of isotopic ratio during one fluid transit time, so the solid can be considered to have a constant (unchanging in time) isotopic ratio over the timescale of fluid transit. This approximation is a useful limiting case because it can be analyzed easily. The general condition whereby the solid phase can be considered to be "stationary" with regard to its isotopic ratio is:

$$MK \gg \frac{\tau_a}{\tau_f}. \quad (7)$$

When Eq. (7) applies, the isotopic evolution of the fluid can be evaluated without regard for the changing isotopic composition of the solid. The ratio τ_a/τ_f is a Damköhler number, and was denoted as N_D by Johnson and DePaolo (1994).

A useful form of Eq. (4c) (also (5a) and (6a)) is that for which the fluid isotopic composition is unchanging in *time*. This form, acquired by setting the time derivative to zero, is useful mainly for situations where Eq. (7) applies

$$\frac{dr_f}{dx} = \frac{RMC_s}{vC_f}[r_s - \alpha r_f] \quad (8)$$

or equivalently,

$$\frac{dr_f}{dx'} = \frac{\tau_a}{\tau_f}[r_s - \alpha r_f]. \quad (9)$$

The solution to these equations is a simple exponential function of distance (Fig. 2). This form will be used below for comparing the fracture model behavior with that of the porous flow model.

2.1.1. Model versus observations: why use the steady state approximation?

In a typical application of the porous flow model to a natural fluid–rock system, the observable parameter (for present purposes) is the change of isotopic ratio with distance in the fluid—dr_f/dx. This information can be deduced, for example, by comparing measurements of fluids pumped from wells along the flow path, or from measurements of fluid emanating from a spring combined with independent knowledge of the initial composition of the water where the aquifer is recharged. By reference to Eq. (4a), one can see that the measurement of dr_f/dx provides a constraint, but it can be interpreted in terms of combinations of the other parameters on the right-hand side of Eq. (4a), or in terms of the time dependence (i.e., dr_f/dt). Geologic systems are likely to evolve on time scales of thousands or hundreds of thousands of years, so in most cases it is not possible to determine dr_f/dt, and in any case the expectation would be that this term is small. A reasonable approach is then to start with the assumption that

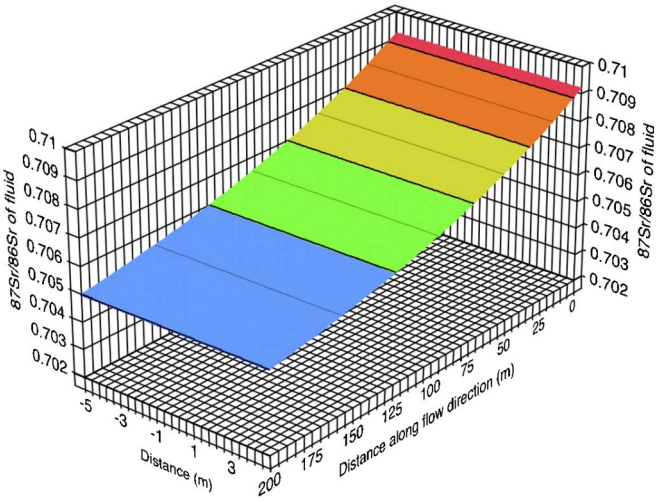

Fig. 2. Graph showing the change of $^{87}Sr/^{86}Sr$ in fluid moving through a rock medium with uniform porosity and permeability. Fluid enters the system with $^{87}Sr/^{86}Sr = 0.7092$ and has a pore velocity of 1 m yr^{-1}. The rock matrix has $^{87}Sr/^{86}Sr = 0.7032$, a porosity of 0.01, and is dissolving and reprecipitating at a rate of $R = 6.7 \times 10^{-7}$ g g^{-1} yr^{-1}. The Sr concentration in the solid is 35 times that in the fluid ($K = 35$). In this model the $^{87}Sr/^{86}Sr$ in the fluid varies only along the direction of flow.

$dr_f/dt = 0$. Likewise, since dr_s/dt is likely to be much smaller than dr_f/dt, it is consistent to assume that $dr_s/dt = 0$ as well. These assumptions then allow one to constrain the combination of parameters on the right-hand side of Eq. (4a), given that the system is not in a transient state. One can then evaluate separately the effect of non-steady state conditions on the deduced parameters (cf. Johnson and DePaolo, 1997b).

Given the steady state assumption, Eq. (8) would then apply. In a typical circumstance, one might have knowledge of the rock isotopic compositions and concentrations so that r_s and C_s are constrained, and measurements of r_f and C_f would be available. In general, α would be known to be unity or could be specified as a function of temperature. The observation (dr_f/dx) would then provide an estimate of the advective "reactive lengthscale" or "reaction length" (La)

$$La = \frac{vC_f}{RMC_s} \approx \frac{q\rho_f C_f}{R\rho_s C_s}. \quad (10)$$

The second approximate equality substitutes the fluid flux (q) for the product $v\phi$, and employs the approximation that $(1 - \phi) \approx 1$. If C_f and C_s are observables, then the data will constrain q/R, since densities can usually be estimated well. Thus, the observations would tend to be converted to estimates of q/R, and in general the observations are aimed at determining fluid flux, fluid velocity, or reaction rates.

In the remainder of the discussion, use of the steady state model is emphasized. This is not meant to imply that all natural systems are at steady state. For the purposes of this presentation, it is a useful approach because it allows for analytical solutions of the equations, and results in a simple formulation that can be easily applied to natural

systems. In addition, it is often a fact that one cannot do better than the steady state assumption as a result of limitations to the characterization of active fluid–rock systems. Where more extensive characterization is available, one may be able to derive more information from it with a more comprehensive model. The simpler model is a way to get a first estimate of system behavior, and is useful as a pedagogical tool.

2.1.2. Conversion to delta and epsilon notation

For stable isotope ratios such as $^{18}O/^{16}O$ the ratios are generally expressed in delta notation where:

$$\delta^{18}O = 1000\left(\frac{^{18}O/^{16}O_{sample}}{^{18}O/^{16}O_{standard}} - 1\right). \tag{11}$$

From this expression it is evident that

$$\partial(\delta^{18}O) = \frac{1000}{^{18}O/^{16}O_{standard}}\partial(^{18}O/^{16}O_{sample}). \tag{12}$$

This relationship can be used to recast Eqs. (4a) and (4b) into the following forms:

$$\frac{d\delta_f}{dt} = -v\frac{d\delta_f}{dx} + RM\frac{C_s}{C_f}[\delta_s - \delta_f - \Delta_{s/f}], \tag{13a}$$

$$\frac{d\delta_s}{dt} = -RK\frac{C_f}{C_s}[\delta_s - \delta_f - \Delta_{s/f}], \tag{13b}$$

where a generalized "δ" is used and $\Delta_{s/f} = 1000\ln\alpha$. These equations involve approximations, but they are adequate for $(\alpha - 1) \ll 1$ and $\delta/1000 \ll 1$. For Nd and Hf, epsilon notation is used, and ε_{Nd} and ε_{Hf} can simply be substituted for δ in Eqs. (13a) and (13b) with $\Delta_{s/f} = 0$.

2.2. The parallel plate fracture model equations

The conceptual model considered here for a fracture-dominated situation consists of a rock system that has parallel plate-like fractures of width "d" and porosity ϕ_f separated by a fixed distance "b" (Fig. 1). Fluid moves through the fractures in the x-direction at a velocity, v_f. The matrix between the fractures is characterized by a (fluid-filled) porosity ϕ_m. Within the matrix, the minerals in the rock exchange isotopes with the pore fluid by dissolving and re-precipitating at a bulk rate "R_m" which is given in grams of solid dissolved (and precipitated) per gram of solid per unit time (e.g., Richter and Liang, 1993; Johnson and DePaolo, 1994). The isotopes in the fluid phase within the matrix block mix with those in the fluid phase in the fractures by diffusion through the pore fluid. It is assumed that solid-state diffusion is negligible, and that there is no matrix fluid flow. The reaction rate, R_m, is assumed to be determined independently of the isotopic exchange; it does not scale with the degree of isotopic disequilibrium.

In the fractured rock system, chemical transport in the fractures needs to be treated separately from the transport in the rock slabs between the fractures. Transport in the fractures is predominantly via fluid advection in the x-direction, and transport in the matrix slabs is by diffusion through the pore fluid in the y-direction. The conservation equation, analogous to Eqs. (1a) and (1b), that describes the evolution of concentration in the fluid moving through the fractures is

$$\phi_f\frac{\partial C_f(x)}{\partial t} = D_v\phi_f\frac{\partial^2 C_f(x)}{\partial x^2} - v_f\phi_f\frac{\partial C_f(x)}{\partial x} + \frac{2D\phi_m}{d}\left(\frac{\partial C_p(x,y)}{\partial y}\right)_{wall}, \tag{14}$$

where D_v is the dispersion coefficient for flow in the fractures; D is the ionic diffusivity in the matrix pore fluid (including tortuosity correction); $C_f(x)$ is the concentration in the fracture fluid, assumed to be uniform across the fracture; $C_p(x,y)$ is the concentration in the matrix pore fluid; ϕ_m and ϕ_f are the matrix and fracture porosities, respectively; v_f is the velocity of the fluid in the fractures in the x-direction.

The third term on the right describes the flux crossing the two walls of the fracture, which depends on the conditions in the matrix, including, as shown below, the fluid–solid reaction rate (R_m) in the matrix. Eq. (14) can represent a single fracture, or a system of identical, equally spaced fractures.

Within the matrix slabs, the pore fluid interacts with the solid matrix by solution–precipitation, and the pore fluid communicates with the fracture fluid by diffusion. The equations that describe the matrix slabs for each element are:

$$\frac{dC_p}{dt} = D\frac{d^2C_p}{dy^2} + R_mM(C_s - KC_p), \tag{15a}$$

$$\frac{dC_s}{dt} = -R_m(C_s - KC_p). \tag{15b}$$

In Eqs. (15a) and (15b) the reaction time constant that applies to the matrix slabs is denoted R_m, to distinguish it from the reaction time constant R that is inferred for a simple porous medium model. For this formulation, it is assumed that the significant concentration and isotopic gradients within the matrix fluid phase are normal to the fracture planes (in the y-direction). The equation for the steady state isotopic ratio in the fracture fluid is obtained using Eq. (3) and the steady state form of Eq. (14) with the dispersion term removed. The result, analogous to Eq. (8) for a porous medium, is

$$\frac{dr_f}{dx} = \frac{2D\phi_m}{v_f\phi_fC_fd}\left[\left(\frac{dC_p^*}{dy}\right)_{wall} - r_f\left(\frac{dC_p}{dy}\right)_{wall}\right], \tag{16}$$

where C_p^* denotes the concentration of one isotope and C_p is the concentration of the other isotope in the matrix pore fluid. For convenience, $y = 0$ is now defined as the location of one fracture wall (the other fracture wall is at $y = -d$), and the matrix slab extends from $y = 0$ to $y = b$. The following equations result in an analytical expression for the isotopic flux at $y = 0$, which is applicable to both fracture walls. Using the chain rule and the relation $C_p^* = r_pC_p$, the term dC_p^*/dy can be eliminated from Eq. (16)

$$\frac{\partial r_f}{\partial x} = \frac{2D\phi_m}{v_f \phi_f C_f d}\left[r_p(0)\left(\frac{\partial C_p}{\partial y}\right)_{y=0} + C_p(0)\left(\frac{\partial r_p}{\partial y}\right)_{y=0} - r_f\left(\frac{dC_p}{dy}\right)_{y=0}\right]. \quad (17)$$

From the condition of continuity at the wall of the fracture, the concentrations must be the same in the fracture and matrix fluid ($C_p(0) = C_f$) and the isotopic ratios must be equal as well ($r_p(0) = r_f$) (Fig. 1b). So the equation for the fracture fluid reduces to

$$\frac{\partial r_f(x)}{\partial x} = \frac{2D\phi_m}{v_f \phi_f d}\left(\frac{\partial r_p(x,y)}{\partial y}\right)_{y=0}. \quad (18)$$

To complete the model formulation it is necessary to have a solution for Eqs. (15a) and (15b), and their analogues for a second isotope, to yield an expression for the isotopic gradient in the pore fluid at the fracture wall.

2.3. Isotopic gradients and transport in the matrix slabs

DePaolo and Getty (1996) treated a problem analogous to that for the matrix slabs that describes the isotopic evolution during metamorphism of layered rocks containing a pore fluid. They obtained solutions for the problem in one dimension, under the condition that there are no concentration gradients in the fluid or solid (i.e., $C_s = KC_m$). Under these conditions, the equations that need to be solved for the pore fluid in the matrix slabs are:

$$\frac{\partial r_p}{\partial t} = D\frac{\partial^2 r_p}{\partial y^2} + R_m MK(r_s - \alpha r_p) \quad (19a)$$

and for the solid matrix in the slabs:

$$\frac{dr_s}{dt} = -R_m(r_s - \alpha r_p). \quad (19b)$$

Solutions to (19a) and (19b) are needed on the interval $y = 0$ to $y = b$, subject to the boundary condition that $r_p(x,0) = r_p(x,b) = r_f(x)$, and an initial condition describing $r_s(x,y)$. DePaolo and Getty (1996) solved these equations for one dimension using Laplace transforms, and generalized them in terms of a Fourier series representation. The solutions give both the instantaneous, quasi-steady state pore fluid isotopic ratio profile for a given solid isotopic profile, and the evolution of both the solid and pore fluid isotope ratio profiles with time.

The starting transverse solid isotopic profile between fractures, at position x along the flow path can be represented in terms of a Fourier series:

$$r_s(y,x) = \alpha r_f(x) + \sum_{n=1}^{\infty} A_n(x)\sin(n\pi y/b). \quad (20)$$

To allow direct comparison to the porous flow situation, it is necessary to specify that there be no isotopic variation in the solid in the y-direction. This specification can be relaxed later to evaluate the long-time evolution of the system. The solid has a uniform isotopic ratio ($=r_s$) on the interval $y = 0$ to $y = b$, if the coefficients are:

$$A_n = \frac{4}{n\pi}[r_s(x) - \alpha r_f(x)], \quad (21)$$

where $n = 1, 3, 5, \ldots, \infty$. Given Eqs. (20) and (21), DePaolo and Getty (1996) show that the steady state fluid isotopic composition is then:

$$r_p(y) = r_f(x) + \sum_{n_{odd}} a_n \frac{4}{n\pi}[r_s(x) - \alpha r_f(x)]\sin(n\pi y)/b, \quad (22)$$

where

$$a_n = \left(1 + n^2\pi^2\frac{L^2}{b^2}\right)^{-1} \quad (23)$$

and L is the diffusive "reaction length," which is applicable to the matrix and defined for each element as:

$$L_i = \left(\frac{D_i}{R_m MK_i}\right)^{1/2}. \quad (24)$$

The diffusive reaction length L_i has the property that (for isotopes of element i) diffusion through the pore fluid is faster than reaction at length scales smaller than L_i, and reaction is faster than diffusion at length scales greater than L_i. Eq. (22) satisfies the boundary conditions: $r_p(x,0) = r_p(x,b) = r_f(x)$. The subscript "$i$" in Eq. (24) denotes that the parameter is element specific. Substituting Eq. (23) into Eq. (22) and rearranging yields the following, which constitutes the solution to Eq. (19a), with the condition that $r_s(x,y)$ is constant

$$r_p(x,y) = r_f(x) + [r_s(x) - \alpha r_f(x)]\frac{4}{\pi} \times \sum_{n_{odd}}\left(1 + n^2\pi^2\frac{L^2}{b^2}\right)^{-1}\frac{1}{n}\sin(n\pi y)/b. \quad (25)$$

The reaction rate is contained in the term L.

The steady state isotopic profiles (Eq. (22)) for the matrix fluid between fractures are shown in Figs. 3 and 4 for different values of the ratio L/b, where here it is assumed that $d \ll b$. When the ratio L/b is significantly greater than unity, diffusion within the matrix pore fluid is fast enough in comparison to the fluid–solid exchange rate that isotopic gradients cannot be maintained between the matrix pore fluid and the fracture fluid. In this case, the matrix fluid has the same isotopic ratio as the fracture fluid at steady state. When L/b is less than one, however, there are significant isotopic gradients in the pore fluid near the fractures. For $L/b \ll 1$, the fracture fluid is not being affected by the exchange in the interior of the matrix slab. The fracture fluid is exchanging isotopes only with a region within a distance of about L of the fracture. The interior of the slab is effectively a "closed system," where the reaction products (the solid precipitates) have the same isotopic ratio as the solid material undergoing dissolution.

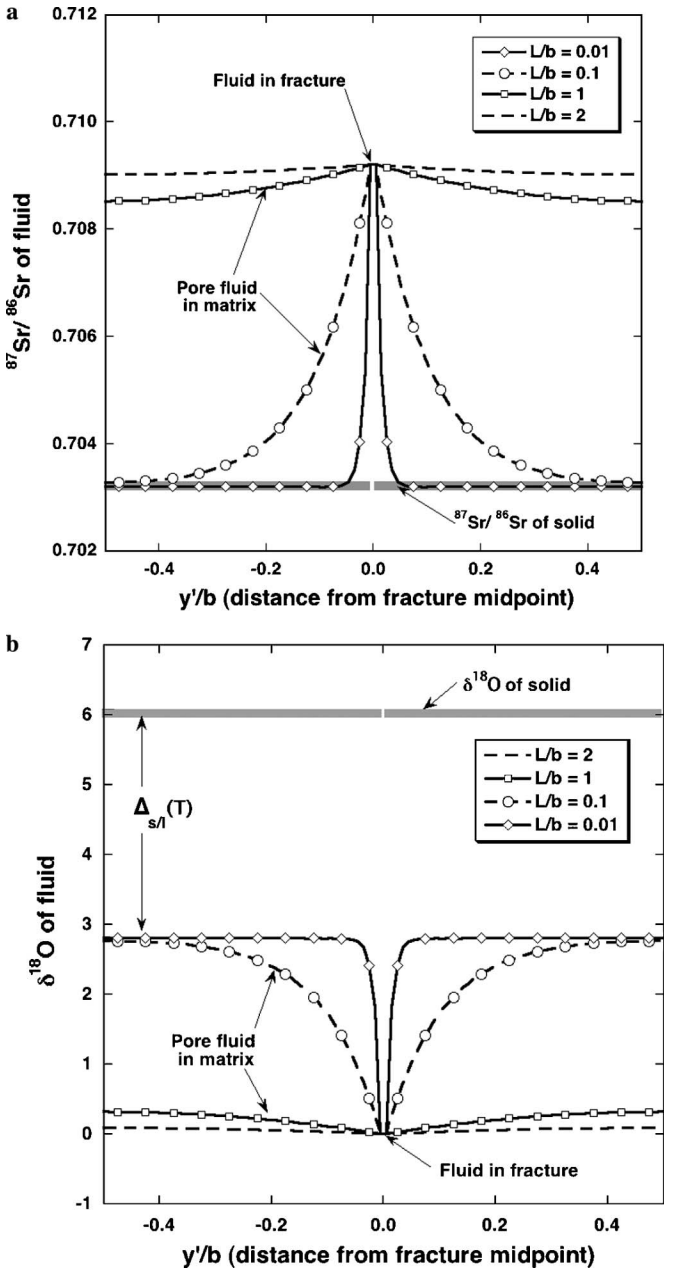

Fig. 3. (a) Calculated profile of Sr isotopic composition of the fluid in the matrix between fractures. The center of the fracture is located at $y' = 0$; adjacent fractures are at $y' = \pm(b + d)$. L is the reaction length. For $L/b \ll 1$, the pore fluid in the interior of the matrix is in isotopic equilibrium with the solid, and there is a steep gradient in isotopic ratio near the fractures. In this situation, most of the dissolution of matrix solid material is followed by reprecipitation of solid with the same isotopic ratio. Only a small amount of the water–rock reaction affects the fluid in the fractures. For $L/b > 1$, the isotopic composition of the pore fluid within the matrix is almost identical to that of the fluid in the fractures. In this case, which corresponds to either a slow rate of reaction or rapid diffusion in the pore fluid, the fluid in the fractures receives the full effect of the reaction with the matrix solid, and the system behaves as if it were a single porosity medium. (b) Analogous to (a) but showing oxygen isotope ratios as $\delta^{18}O$. The isotopic composition of matrix pore fluid is determined by the isotopic composition of the solid combined with the solid–fluid fractionation factor α. This example assumes a value of $\alpha = 1.0032$ (or $\Delta = 3.2$).

2.4. Steady state solution for the parallel fracture model

Differentiating and evaluating Eq. (22) at $y = 0$ (the position of the fracture wall) yields for the isotopic gradient in the matrix pore fluid at the fracture wall

$$\left(\frac{dr_p(x,y)}{dy}\right)_{y=0} = \frac{4}{b}[r_s(x) - \alpha r_f(x)] \sum_{n_{odd}} \left(1 + n^2\pi^2 \frac{L^2}{b^2}\right)^{-1}. \tag{26}$$

Substituting this result into Eq. (18) gives:

$$\frac{dr_f(x)}{dx} = \frac{8D\phi_m}{v_f\phi_f bd}[r_s(x) - \alpha r_f(x)] \sum_{n_{odd}} \left(1 + n^2\pi^2 \frac{L^2}{b^2}\right)^{-1}. \tag{27}$$

Eq. (27) is the explicit version of Eq. (18) and describes the steady state fluid isotopic variation with distance for the dp, parallel fracture model.

A useful next step is to compare the result for the fracture (or dp) model to that for the sp model. Dividing Eq. (27) by Eq. (8) yields:

$$\frac{(dr_f/dx)_{dp}}{(dr_f/dx)_{sp}} = \frac{8D\phi_m vC_f}{(v_f\phi_f bd)RMC_s} \sum_{n_{odd}} \left(1 + n^2\pi^2 \frac{L^2}{b^2}\right)^{-1}. \tag{28}$$

If we assume that R, the reaction time constant that would be attributed to a simple porous medium is the same as R_m, the reaction time constant that applies to the matrix slabs in the dp model, then Eq. (28) can be simplified because $DC_f/RMC_s = L^2$. Multiplying through by b/b yields:

$$\frac{(dr_f/dx)_{dp}}{(dr_f/dx)_{sp}} = \frac{\phi_m bv}{v_f\phi_f d} 8\frac{L^2}{b^2} \sum_{n_{odd}} \left(1 + n^2\pi^2 \frac{L^2}{b^2}\right)^{-1}, \tag{29}$$

which is equivalent to:

$$\frac{(dr_f/dx)_{dp}}{(dr_f/dx)_{sp}} = \frac{\phi_m bv}{v_f\phi_f d} \tanh\frac{2L}{b}. \tag{30}$$

To complete this comparison we assume that the fluid flux is the same for each model. For equal fluid fluxes:

$$v_f\phi_f d = v\phi_m(b + d). \tag{31}$$

Using this expression in Eq. (30) yields:

$$\frac{(dr_f/dx)_{dp}}{(dr_f/dx)_{sp}} = \frac{b}{b + d} \tanh\frac{2L}{b}. \tag{32}$$

In most cases, d is much smaller than b, and the term $b/(b + d)$ is close enough to unity to ignore (Fig. 5). The curves in Fig. 5 show the difference between a situation where fluid is flowing through a simple porous medium with a reaction rate R ($=R_{sp}$), versus a system where the fluid is flowing only through fractures but the reaction rate in the matrix slabs, R_m, is equal to R.

As noted above, the observed value—dr_f/dx—is typically interpreted as a measure of R/q. To a very good approximation (Fig. 5), Eq. (32) states that for $L/b > 1$, the value of R/q that is deduced assuming that a sp model applies is no different from that inferred using the dp model. In this

limit, which is applicable for closely spaced fractures, slow reaction rates, and fast-diffusing species with high solubility, the system behaves (at least as far as the isotopic composition of the fluid is concerned) as if it had a sp and the presence of the fractures and fracture flow makes no difference to the isotopic effects. When $L/b < 1$, the apparent R/q that is obtained assuming that the sp model applies, is systematically smaller than the actual value R_m (in the matrix slabs) divided by the volume-averaged fluid flux. For $L/b < 0.3$, the apparent R/q is proportional to L/b and lower than the actual (R_m/q) by a factor of $2L/b$. The condition $L/b \ll 1$ is likely to be applicable for widely spaced fractures, high reaction rates, and dissolved species with low solubility. Note that because L is proportional to $R_m^{-1/2}$, the inferred reaction rate will scale as b^2, and for $L < 0.3b$:

$$\frac{R_m}{R_{sp}} = \left(\frac{b}{2L_{sp}}\right)^2, \tag{33}$$

where L_{sp} is the reaction length calculated with R_{sp} as the reaction rate.

3. Examples and applications

3.1. Sr isotopes; seawater in fractured basalt

Figs. 2 and 4a and b constitute an example of the results of Eqs. (25) and (27) applied to a hypothetical system of identical parallel equidistant fractures. The concentration and isotopic ratio values used for the example would apply to seawater (8 ppm Sr; $^{87}Sr/^{86}Sr = 0.7092$) passing through fractured oceanic basalt with 280 ppm Sr and $^{87}Sr/^{86}Sr = 0.7032$. Fig. 2 shows the result for simple porous flow through a medium with $\phi = 0.01$, $R = 6.7 \times 10^{-7}$ yr^{-1}, and a pore velocity of $v = 1$ m yr^{-1}. The essential observation in this hypothetical system is that the water emerges with an isotopic ratio (about 0.7050) that is substantially lower than the value in the input water. Given that the distance is known (as well as porosity and the concentrations), this isotopic change corresponds to $R/v = 6.7 \times 10^{-7}$ m^{-1} (or $R/q = 6.7 \times 10^{-9}$ m^{-1}).

Fig. 4a shows an example of an equivalent system where all of the flow is confined to fractures that are 0.1 m in width ($\phi_f = 1$) and separated by 10 m. Since the flow is confined to 1/101 of the cross sectional area of the rock, for the same fluid flux, the fluid velocity in the fractures is 101 m yr^{-1}. In this case, to have the water emerge from the system with the same isotopic ratio ($^{87}Sr/^{86}Sr = 0.705$), it is necessary to have the reaction rate in the matrix slabs be much higher ($R_m = 10^{-5}$ yr^{-1}), about 15 times higher than the rate for the porous flow (sp) case. The model indicates that the pore fluid in the matrix slabs is effectively in isotopic "equilibrium" with the rock ($^{87}Sr/^{86}Sr = 0.7032$), and there is a narrow zone adjacent to the fracture where there is a large gradient in isotopic ratio of the dissolved Sr. For this example, L for Sr is 0.33 m, which is much smaller than the 10 m fracture spacing. The value of R/v_f for this example is about 10^{-7}, which is different from the value that would be inferred from the porous flow model by only a factor of 1.5.

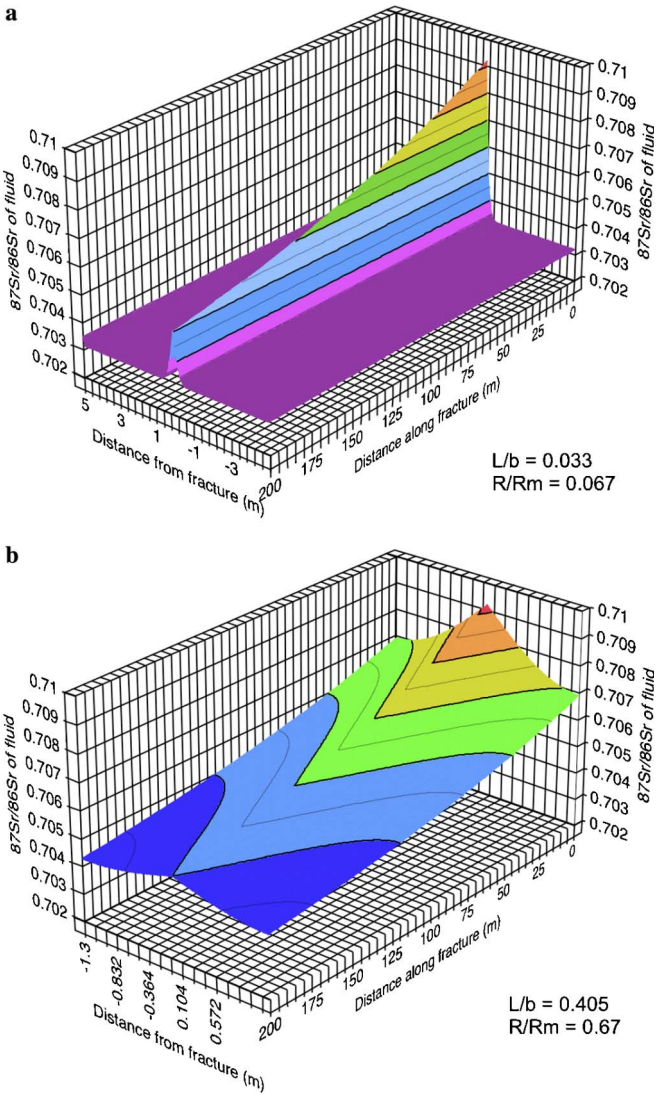

Fig. 4. (a) Simulation of Sr isotope ratios in pore fluid within and surrounding a fracture for conditions where $L/b \ll 1$. The fracture fluid exiting the system at $x = 200$ m has $^{87}Sr/^{86}Sr = 0.705$, as in the single porosity example shown in Fig. 2. Fluid enters the fracture at $x = 0$ with $^{87}Sr/^{86}Sr = 0.7092$. The fracture is 0.1 m wide ($\phi_f = 1$) and the fracture spacing is 10 m. The fluid in the fracture has a velocity of 101 m yr^{-1} so that the fluid flux is identical to that of the example in Fig. 2. The rock matrix has $^{87}Sr/^{86}Sr = 0.7032$, a porosity of 0.01, and is dissolving and reprecipitating at a rate $R = 10^{-5}$ g g^{-1} yr^{-1} ($L = 0.33$ m). The Sr concentration in the solid is 35 times that in the fluid ($K = 35$). In this model the $^{87}Sr/^{86}Sr$ in the pore fluid within the matrix has large gradients near the fracture and is equal to the rock value at distances greater than about 0.5 m from the fracture. (b) Simulation of Sr isotope ratios in pore fluid within and surrounding a fracture for conditions where $L/b \approx 1$. The fracture fluid exiting the system at $x = 200$ m still has $^{87}Sr/^{86}Sr = 0.705$. Fluid enters the fracture at $x = 0$ with $^{87}Sr/^{86}Sr = 0.7092$. The fracture is 0.1 m wide and the fracture spacing is 2.6 m. The fluid in the fracture has a velocity of 27 m yr^{-1}. The rock matrix has $^{87}Sr/^{86}Sr = 0.7032$, a porosity of 0.01, and is dissolving and reprecipitating at a rate $R = 10^{-6}$ g g^{-1} yr^{-1} ($L = 1.06$ m). The Sr concentration in the solid is 35 times that in the fluid ($K = 35$). In this model the $^{87}Sr/^{86}Sr$ in the pore fluid within the matrix has gradients throughout the matrix volume.

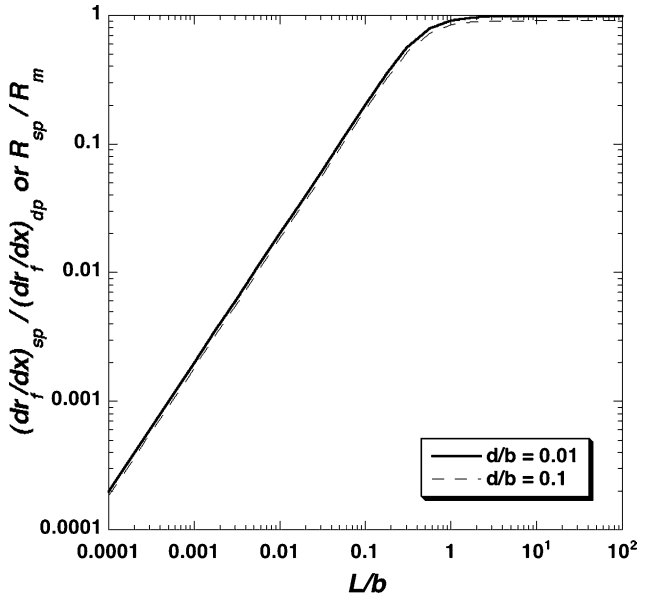

Fig. 5. Calculated dual porosity effect for fluids moving in fractures and communicating with matrix blocks by fluid-phase diffusion. The vertical scale can be interpreted in terms of the rate of change with distance of the isotopic ratio of the fluid (dr_f/dx), or the inferred dissolution or reaction rate of the solid matrix. The parameter R_m is the solution–precipitation time constant in the matrix blocks, and R_{sp} is the apparent reaction time constant that is sensed by fluid moving in the fractures under steady state conditions and under the assumption that the system behaves as a simple porous medium. When L/b is greater than unity, there is no difference between the reaction rates, which means that the same result will be obtained whether the system is modeled as a fractured medium or a simple porous medium. When L/b is less than about 0.3, the reaction rate as sensed by the fracture fluids is lower than that in the matrix blocks by a factor of $2L/b$.

A third example (Fig. 4b) shows a case where there is a much smaller difference between L for Sr (about 1 m) and the fracture spacing (2.6 m). The model parameters are adjusted to achieve the same isotopic ratio (0.705) in the fluid emerging from the fractures. In this example, the pore fluid in the matrix slabs is not identical in isotopic ratio with the rock because diffusion within the pore fluid competes with the exchange of Sr between solid and fluid. The pore fluid has isotopic gradients everywhere and in general does not have the same isotopic composition as the fracture fluid. For the same value of R/q, the reaction rate for this case is 10^{-6} yr^{-1}, about 1.5 times the reaction rate for the sp case. The fracture width is such that the fracture fluid velocity is 27 m yr^{-1} to achieve the same fluid flux. The ratio R/v_f for this example is about 2×10^{-7} m^{-1}.

The examples illustrate the behavior of the model for a single element. One interesting aspect of the model is that the reaction length (L) is not the same for all elements. The difference between elements is mainly a result of differences in C_s/C_f (or K), and to a lesser extent differences in the ionic diffusivity D. The models also hint at the difference in the effects that will accrue to the solid matrix if the system operates long enough to have significant isotopic changes in the solid. In all three models, the bulk solid isotopic ratio will tend toward the fluid isotopic ratio with time. For the porous flow model, the gradients in fluid isotopic composition are only longitudinal (in the direction of flow), and hence the altered solid will have a similar characteristic. In the model shown in Fig. 4a, however, isotopic alteration of the solid will be confined to the small region adjacent to the fractures, because that is the only place where the fluid isotopic ratio departs from that of the solid. The model of Fig. 4b is an intermediate case, where there will be pervasive isotopic modification of the solid, but it will be more non-uniform than in the simple porous flow case. Perhaps more importantly, secondary minerals forming in the reacting solid matrix will have the isotopic ratio of the pore fluid. So the isotopic distributions shown in Figs. 4a and b also represent maps of the isotopic ratios of actively forming secondary alteration minerals. In the case represented by Fig. 4a, for example, the secondary minerals far from the fractures have isotopic compositions that are little different from the unaltered rock, whereas those close to the fracture have isotopic compositions closer to that of the fluid in the fractures. In general, the isotopic differences between secondary minerals close to fractures and those far from fractures may be a good indicator of L/b.

3.2. Restrictions of the steady state model

The equations derived above are applicable to a system at "steady state," the definition of which requires explanation as there are three timescales involved. One timescale is associated with advection—the time it takes for fluid flowing in the fractures to traverse the system. A second timescale relates to the diffusive transport of the isotopes between the matrix slabs and the fractures, through the medium of the matrix pore fluid. The third timescale is defined by the reaction rate constant.

The reaction timescale (R^{-1}) is typically long in comparison to the other timescales, which is the basis for the assumption that the solid phase undergoes negligible change over the timescale of fluid transport. The steady state that the model describes is one where both the matrix pore fluid and the fracture fluid have reached a state where their isotopic compositions are steady (in the sense that their rate of change with time is only the much longer timescale R^{-1}) and defined by the model input parameters. Considering the diffusive regime within the matrix fluid, the time required to reach the steady-state relation between fluid and solid (Eq. (22)), is (DePaolo and Getty, 1996):

$$\tau_i = \left(\frac{D_i}{b^2} + \frac{D_i}{L_i^2}\right)^{-1} = \left(\frac{D_i}{b^2} + RMK_i\right)^{-1}. \quad (34)$$

The examples presented above in Figs. 4a and b can be used to illustrate the relative values of the three timescales. For the case of Fig. 4a, the reaction timescale is 10^5 years; on this timescale, the isotopic composition of the solid matrix changes. The advection time scale is about 2 years. The

diffusive timescale as given by Eq. (34) is about 11 years. Therefore, it is to be expected that the system would effectively reach steady state after about 30 years. Thereafter, the system would evolve very slowly on the 10^5-year timescale of the solid matrix. In 30 years there is virtually no change in the isotopic composition of the solid. Only after several thousand years would there be significant changes in the isotopic composition of the solid, and those would be restricted to the region adjacent to the fracture. For the example shown in Fig. 4b, the reaction time scale is 10^6 years, the fluid advection timescale is about 4 years, and the diffusion timescale is 95 years. In this hypothetical system, it would take the fluids about 300 years to reach steady state, and it would require 10,000–100,000 years before the solid isotopic ratios changed significantly. In real systems the advection distance may be 10–100 times longer than these examples, but the advection time would still be short relative to the reaction timescale.

Externally imposed changes affecting the fracture fluids, either in terms of fluid velocity or isotopic composition, that occur on time scales that are long in comparison to τ_i are adequately described by the model. Changes affecting the fracture fluids that occur on time scales similar to or smaller than τ_i are not. Because the time required for the matrix to reach a new steady state differs from element to element, during transient fast flow events the dp effects will be evident as a form of hysteresis exhibited in the change of one fluid isotopic ratio relative to another. For fracture spacings of 0.1–10 m, the magnitude of τ_i is generally in the range 10^{-3}–10^4 years and can differ by orders of magnitude among different elements (see Fig. 5).

3.3. Adding a second element with isotopic variations

As noted above, the diffusive timescale depends on both D and K (as well as b and R) and hence varies with the element being considered. Another hypothetical example illustrates how this works for Sr and O isotopes (Fig. 6). The distribution of pore fluid Sr isotope ratios is similar to that shown in Fig. 4a, but in this example a slightly higher reaction rate is used. The value of L_{Sr} is 0.21 m, which is much smaller than the fracture spacing of 10 m, so there are large isotopic gradients adjacent to the fracture, but elsewhere there is virtually no difference in isotopic ratio between the fluid and the solid. Hence, the fracture fluid is not sensing most of the fluid–rock interaction. In contrast to Sr, the reaction length for oxygen, L_O, is 4.4 m, or about half the spacing between the fractures. For oxygen, the pore fluid in the matrix slabs is only slightly different from the fracture fluid in isotopic composition, so for oxygen, the fracture fluid is sensing most of the fluid–rock interaction. The difference in reaction length is due to the higher diffusivity of O (self-diffusion of H_2O), and the fact that C_s/C_f is 35 for Sr but only about 0.55 for O. The pore fluid in the oxygen case does not have the $\delta^{18}O$ that would represent equilibrium with the solid. The equilibrium $\delta^{18}O$ value is assumed for the calculation to be +2.8, the approximate value for water in equilibrium with typical igneous rock (actually feldspar) with $\delta^{18}O = +6$, at about 350 °C.

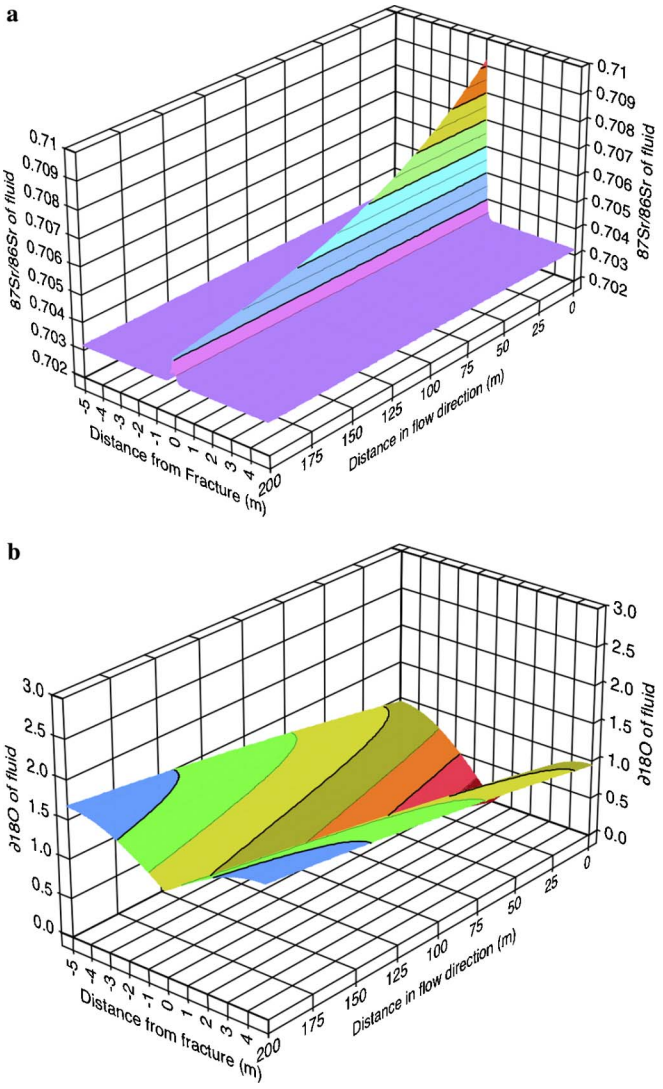

Fig. 6. Comparison of Sr and O isotopes in pore fluids for a hypothetical fluid–rock system. (a) Sr isotope ratios in pore fluid within and surrounding a fracture. Parameters are the same as those for Fig. 4a except for the reaction rate $R = 2.5 \times 10^{-5}$ g g^{-1} yr^{-1} ($L_{Sr} = 0.21$ m). (b) Simulation of O isotopes (as $\delta^{18}O$) for the same system as shown in (a). Fluid entering the system at $x = 0$ has $\delta^{18}O = 0$. Fluid in equilibrium with the rock matrix has $\delta^{18}O = +2.8$. The reaction length for oxygen is $L_O = 4.44$ m.

The difference between porous flow and the fracture flow models is illustrated in another way in Fig. 7, which shows the evolution of $^{87}Sr/^{86}Sr$ and $\delta^{18}O$ in the fluid as it traverses the system. For porous flow, the $^{87}Sr/^{86}Sr$ ratio changes rapidly with almost no change in $\delta^{18}O$. For fracture flow, there is a much larger shift in $\delta^{18}O$, which is a result of the fact that the fluid oxygen is interacting with much more of the rock volume than is the fluid Sr.

4. Time evolution of the solid

The non-uniformity of isotopic ratios in the fluid phase that is generated by the pore fluid diffusive transport

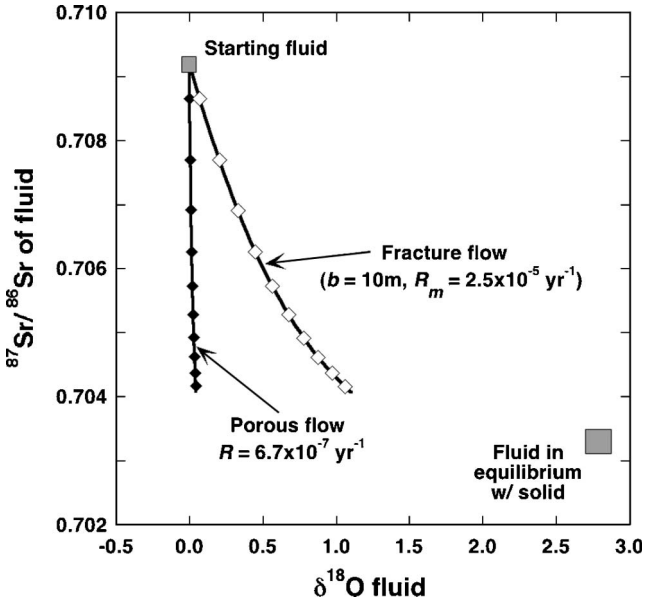

Fig. 7. Contrasting trajectories for porous flow and fracture flow for Sr and O isotopes. The curves are based on the simulation shown in Fig. 6. Because of the larger reaction length for oxygen in comparison to Sr, there is a proportionally larger shift in O isotopes for the fracture flow case.

creates a non-uniform response in the solid as it slowly changes isotopic composition due to exchange with the fluid phase. Some aspects of this effect are discussed by DePaolo and Getty (1996) with reference to layered metamorphic rocks. The exact solution of this part of the problem is beyond the scope of this paper, but an approximate expression can be used to evaluate the effects.

The essential point derives from Eq. (15b). The rate of change of the isotopic ratio of the solid is proportional to the difference between the equilibrium value for the solid (which is determined by the local fluid isotopic composition) and the actual solid isotopic composition. Referring to Fig. 5, since the interior of the matrix slabs are in isotopic equilibrium with the fluid for Sr isotopes, there will be no change with time in the solid phase $^{87}Sr/^{86}Sr$. However, since the interior of the matrix slabs are not in equilibrium with the pore fluid for O isotopes, there will be significant change with time in the solid phase $\delta^{18}O$. Consequently, the relative magnitude of Sr and O isotopic shifts in the solid are spatially highly variable. Adjacent to the fractures, both Sr and O isotopes in the solid change with time, but in the center of the matrix slabs, only the O isotopic ratios can change. If the system persists for a long enough time, eventually the interiors of the slabs will change with respect to Sr isotopes as well.

The solid phase isotopic profile (normal to the fractures) evolves with time (approximately) according to (DePaolo and Getty, 1996)

$$r_s(x,y,t) = \alpha r_f(x,0) + \sum_{n_{odd}} \frac{4}{n\pi}[r_s(x,0) - \alpha r_f(x,0)]e^{-\lambda_n t} \times \sin(n\pi y/b), \quad (35)$$

where

$$\lambda_n = \frac{R}{1 + b^2/n^2\pi^2L^2}. \quad (36)$$

Eq. (35) will be a reasonable estimate of the solid evolution as long as the local fracture fluid isotopic ratio does not change too drastically over the timescale to which it is applied. The pore fluid isotopic ratio is described (approximately) by

$$r_p(x,y',t) = r_f(x,0) + [r_s(x,0) - \alpha r_f(x,0)]\frac{4}{\pi} \times \sum_{n_{odd}} \left(1 + n^2\pi^2\frac{L^2}{b^2}\right)^{-1} \frac{e^{-\lambda_n t}}{n} \sin(n\pi y/b). \quad (37)$$

Examples of the solid isotope effects are shown in Figs. 8 and 9, which are calculated using the same parameters as in Fig. 6. The Sr shifts for the bulk solid are limited to the region close to the fracture. In contrast, there is pervasive change of the solid $\delta^{18}O$, although the shifts are slightly larger closer to the fracture. When the Sr and O isotopic ratios of the bulk solids are plotted against one another (Fig. 9), the result is a pattern that cannot be interpreted correctly except with the dp model. Relative to a simple batch reactor, where the rock and the initial fluid are allowed to equilibrate at the prescribed temperature, the matrix slab interiors are not shifted enough in $^{87}Sr/^{86}Sr$, and the near-fracture samples are shifted far too much.

5. Estimating fracture spacing

The diffusive reaction length, L, has a large range among elements with natural isotopic variability (Fig. 10). The reaction length scales as $(R_m/\phi)^{-1/2}$, and the differences between elements are largely due to solubility limitations. The figure shows two curves for Sr, one for seawater systems, where Sr has a relatively small value of K (or C_s/C_f), and one for meteoric water systems, where Sr has a larger value of K. The elements U and Nd have generally short reaction lengths due to low solubility, and O and H have large reaction lengths because they are the major constituents of water, and particularly in the case of H, rocks have relatively little. Hydrogen is in fact a special case that does not conform to some of the simplifications made in the model discussion above. The K value for hydrogen is typically of order 10^{-2}, so MK is not much larger than unity, and the rock δD values can sometimes shift faster than those of the fluid. This characteristic was used to advantage by Taylor (1974) and Magaritz and Taylor (1976) to estimate the $\delta^{18}O$ of meteoric fluids in fossil hydrothermal systems (see also Criss, 1999).

For most natural conditions it may be possible to find elements with L values that are both smaller and larger than the likely fracture spacing. For any two elements, the ratio of the diffusive reaction lengths is

$$\frac{L_i}{L_j} = \left(\frac{D_iK_j}{D_jK_i}\right)^{1/2}. \quad (38)$$

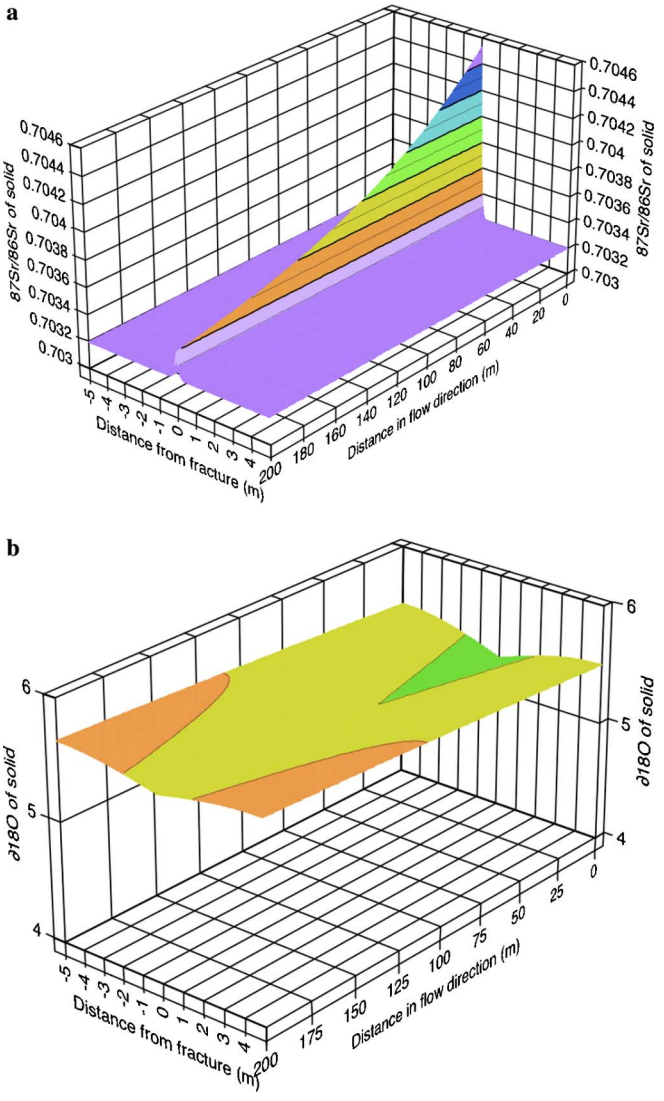

Fig. 8. Isotopic shifts in the *bulk* solid matrix for (a) Sr and (b) oxygen, generated by 10,000 years of exchange with conditions described by the model shown in Fig. 6. The initial state of the solid is uniform isotopic values of $^{87}Sr/^{86}Sr = 0.7032$ and $\delta^{18}O = +6$. These figures are calculated with the approximate formula given in Eq. (35) of the text. The $^{87}Sr/^{86}Sr$ ratios in the secondary minerals, rather than the bulk rock, will closely approximate the values shown for the fluid in Fig. 6a. The $\delta^{18}O$ of secondary minerals will be approximately 2.8‰ higher than the values shown for fluid in Fig. 6b.

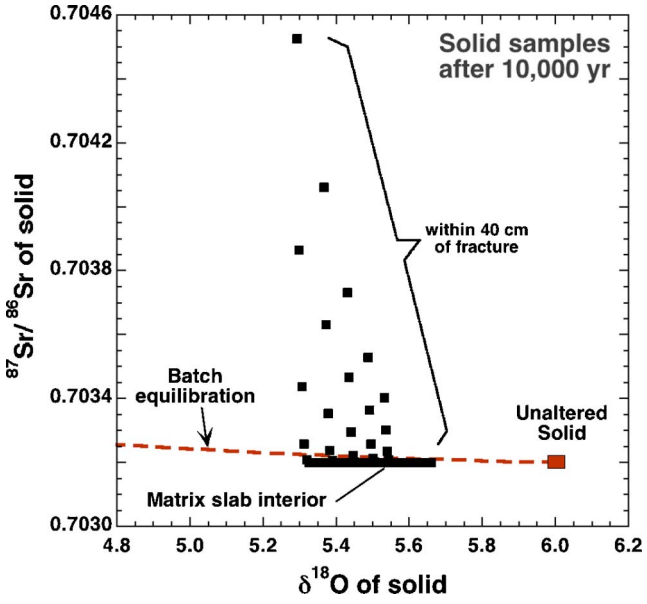

Fig. 9. Model output data from Fig. 8 plotted as $^{87}Sr/^{86}Sr$ versus $\delta^{18}O$. The points plotted represent values at each of the nodes in the simulation. In the matrix slab interiors, the O isotope ratios of the solid samples is shifted significantly after 10,000 years, but there is virtually no change in the Sr isotopic composition. For samples from near the fractures, the O isotope effects are similar to those in the slab interiors, but the Sr isotopes are much more strongly affected.

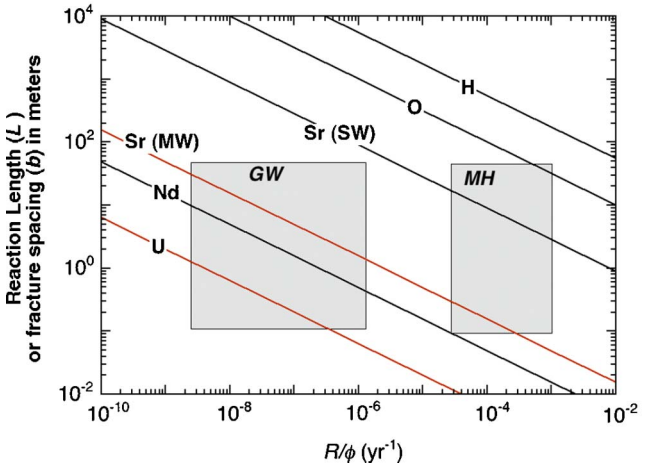

Fig. 10. Estimated diffusive reaction length (L; Eq. (24)) versus R/ϕ for several elements with naturally varying isotopic compositions. Squares show the expected values of R/ϕ and fracture spacing for typical groundwater systems (GW) and (postulated) for meteoric–hydrothermal systems hosted by volcanic rocks (MH). For a typical hydrothermal system ($R/\phi = 0.001$ yr^{-1}, $b = 1$ m), O and H isotopes typically behave as though the system has a single porosity (i.e., $L/b > 1$), but Sr, C, Nd, and U isotopes will be affected by the sluggishness of diffusive transport within the matrix (i.e., $L/b \ll 1$).

If the fracture spacing has a value that is larger than the L for one of the elements, comparison of isotopic effects of two or more elements can theoretically yield information about the fracture spacing.

One way to analyze the dp effect is to plot the isotopic shift in one element against that of another, as is done in Fig. 7. This can be generalized by combining Eqs. (8) and (32), with the result:

$$\left(\frac{dr_{fi}}{dr_{fj}}\right)_{dp} = \frac{(dr_{fi}/dx)_{dp}}{(dr_{fj}/dx)_{dp}} = \frac{C_{si}/C_{fi}}{C_{sj}/C_{ji}} \frac{\tanh\frac{2L_i}{b}}{\tanh\frac{2L_j}{b}}. \quad (39)$$

There are three general cases. In the case that both L_i and L_j are larger than b, then the sp model is retrieved, and the ratio of isotopic shifts is dependent only on the concentration terms. In the case that both $(L_i/b)^2$ and $(L_j/b)^2$ are much smaller than one, then the result is:

$$\left(\frac{dr_{fi}}{dr_{fj}}\right)_{dp} = \frac{C_{si}/C_{fi}}{C_{sj}/C_{ji}} \frac{L_i}{L_j} = \left(\frac{C_{si}/C_{fi}}{C_{sj}/C_{ji}} \frac{D_i}{D_j}\right)^{1/2}. \quad (40)$$

For this case, the ratio of the isotopic shifts is not dependent on the fracture spacing, but it requires that the fracture spacing be significantly larger than the larger of the two values of L. In the third case, if $L_j \geqslant b$, and L_i is significantly smaller than b, then:

$$\left(\frac{dr_{fi}}{dr_{fj}}\right)_{dp} = \frac{C_{si}/C_{fi}}{C_{sj}/C_{fj}} \tanh\frac{2L_i}{b}. \quad (41)$$

In this case, the isotopic shifts provide an estimate of the fracture spacing.

For illustration, consider further the evolution of the isotopes of oxygen ($\delta^{18}O$) and strontium ($^{87}Sr/^{86}Sr$) in a geothermal fluid as it passes through rocks of different isotopic composition. In a typical geothermal system at a temperature of 350 °C, the value of α is about 1.003 ($\Delta = 3$), and the parameters given in Fig. 11a might apply if the fluid phase is composed of meteoric water. The limiting values of $(dr_{fSr}/dr_{fO})_{dp}$ are about 6 (Eq. (40)), and 167 (Eq. (39)). The reaction length for Sr, assuming $R = 10^{-4}\,yr^{-1}$, $\phi = 0.01$, and $\rho_s/\rho_f = 2.5$, would be $L_{Sr} = 4$ cm, and the value for O would be $L_O = 1.5$ m. The ratio–ratio trajectories, calculated from Eqs. (8) and (32) for both Sr and O, are shown in Fig. 11a for fracture spacings b of 0.01–10 m. For closely spaced fractures ($b \leqslant 0.05$ m), the large difference in K_i values between O and Sr results in large shifts of $^{87}Sr/^{86}Sr$ with negligible shifts in $\delta^{18}O$. However, for the larger fracture spacings, there are much larger shifts of $\delta^{18}O$ associated with the same shift of $^{87}Sr/^{86}Sr$. The exact trajectory is sensitive to fracture spacing for b between 0.1 and 10 m for this example. For spacing greater than 10 m, both Sr and O isotopic exchange is matrix diffusion limited (Eq. (40)), and hence there is no further dependence on fracture spacing.

Fig. 11b shows the apparent reaction rate for each element as a function of fracture spacing using the same parameters as those for Fig. 11a. As the fracture spacings increase, the apparent reaction rate decreases (as in Fig. 5), but the difference between the apparent and actual reaction rates is larger for Sr than for O. Another conclusion from Fig. 11b is that oxygen isotopes in the fluid can be treated adequately with a sp model as long as the fracture spacing is less than 4 m. However, for Sr isotopes, the fracture spacing would need to be less than 0.1 m for a sp model to apply.

Fig. 11c shows the response time of the reactive-diffusive system in the matrix slab (Eq. (34)). At small fracture spac-

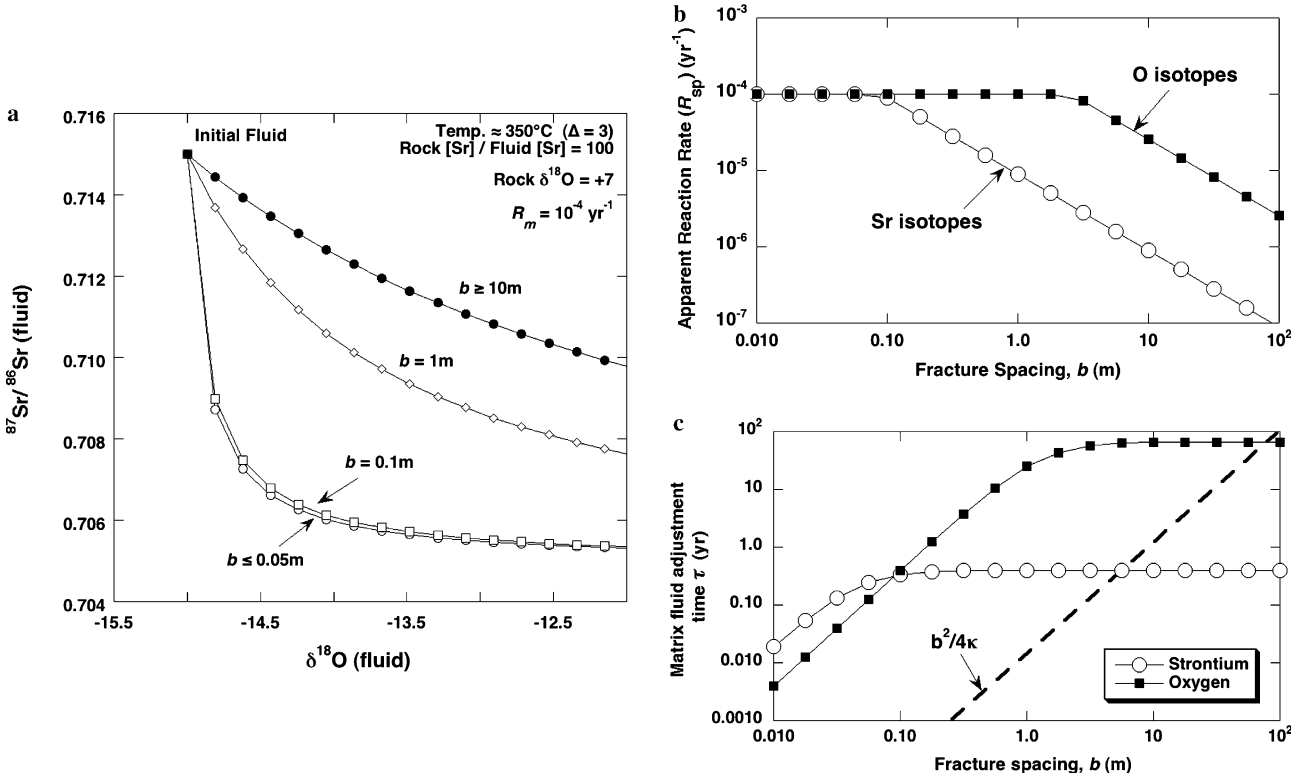

Fig. 11. (a) Example calculation showing the matrix diffusion effects on the relative shifts of $^{87}Sr/^{86}Sr$ and $\delta^{18}O$ values of fluids in a hypothetical continental meteoric-hydrothermal system where the initial water has high $^{87}Sr/^{86}Sr$ and low $\delta^{18}O$. For the parameters given, the trajectories of changing isotopic composition for the fluid depend on the fracture spacing. The single porosity trajectory applies for $b \leqslant 0.05$ m. For increasing fracture spacing up to $b = 10$ m, the $^{87}Sr/^{86}Sr$ shifts decrease relative to the $\delta^{18}O$ shifts, causing the calculated trajectory to deviate substantially from the single porosity case. (b) Relationship between fracture spacing and apparent fluid–rock exchange rate (R_{sp}) for Sr and O isotopes. (c) Characteristic time for reestablishment of steady state conditions in the matrix slabs following a perturbation of the system. For fracture spacing $b < L$, the adjustment time scales as b^2, but for $b > L$, the adjustment time is independent of b (Eq. (34)). Shown for comparison is the thermal response time. The relative values of the O, Sr, and thermal response times change systematically for fracture spacing between 0.01 and 100 m.

ing the timescale is determined by the fracture spacing, whereas for large fracture spacing the timescale is dependent only on L_i. For the model system, the Sr and O timescales diverge substantially at larger fracture spacing, so significantly different behavior should be observed if there are fluctuations in the system, such as variations in flow velocity or variations in the initial isotopic ratio of the fluid entering the system.

6. Groundwater ages—Sanford model

The model described here is analogous in some ways to the model of Sanford (1997) for the effects of diffusive exchange of dissolved carbon between fracture fluids and stagnant matrix fluid. In much the same way, Sanford developed equations for a steady-state system and ignored the effects of longitudinal dispersion in the fractures. However, his equations do not account for exchange between the matrix solid and the pore fluid, as is done for carbon by Maloszewski and Zuber (1991), so they are applicable mainly to non-carbonate bearing rocks. Sanford's equations are reproduced here using the present notation, and modified slightly to account for the matrix porosity, which he did not explicitly treat. These equations are a necessary complement to the model presented above, because radionuclides are typically used to estimate flow velocities (or equivalently, water "age") and hence can be an integral part of any estimate of the flow and transport in a fluid–rock system

The result of the Sanford steady state model can be expressed as:

$$\frac{t_u}{t_c} = 1 + \frac{2L_r}{d}\tanh\frac{b}{2L_r}, \tag{42}$$

where t_u is the observed (uncorrected) radiocarbon age of the water, t_c is the corrected (true) age of the water, and L_r is the radiocarbon decay length (analogous to the diffusive reaction length)

$$L_r = \left(\frac{D_C\phi_m}{\lambda}\right)^{1/2}. \tag{43}$$

Eq. (43) includes the matrix porosity [ϕ_m, a term that was left out of the equations of Sanford (1997)], the ionic diffusivity of dissolved carbon (CO_3^{2-} and HCO_3^-), and the decay constant of ^{14}C ($\lambda = 1.21\times10^{-3}\,yr^{-1}$). For water at 25 °C, the diffusivity of dissolved carbon is about $0.03\,m^2\,yr^{-1}$, so for matrix porosity of 0.01–0.1, L_r takes on values of 0.5–1.5 m.

There are two limiting cases for Eq. (42). For large fracture spacing ($b' > 2L_r$), Eq. (42) reduces to:

$$\frac{t_u}{t_c} = 1 + \frac{2L_r}{d}. \tag{44}$$

For small fracture spacing ($b < L_r$), the result is simply:

$$\frac{t_u}{t_c} = 1 + \frac{b}{d}. \tag{45}$$

These equations would also apply to other radionuclides used in groundwater dating (e.g., ^{36}Cl, ^{3}H), and in a manner similar to that illustrated for Sr and O above, the differences in decay lengths could be used to estimate fracture spacing. For $\phi_m = 0.01$–0.1, the decay length for ^{36}Cl ($\lambda = 2.3\times10^{-6}\,yr^{-1}$) is about 16–50 m, and the decay length for tritium ($\lambda = 0.057\,yr^{-1}$) is about 0.2–0.6 m.

7. Application to natural fluid–rock systems

7.1. Groundwater ages and rock weathering rates

Isotopic data on groundwater can be used to infer weathering rates for the host rocks of aquifers, and can give information that cannot come from chemical concentration data alone (e.g., Johnson and DePaolo, 1997a,b; Johnson et al., 2000). Two recently reported data sets are analyzed here in terms of the fracture–matrix model presented. These examples illustrate some of the complexities inherent in evaluating fluid isotope ratios in fractured-rock aquifers.

The first example involves seawater that is flowing through basalt of the island of Hawaii in the region of Hilo (Fig. 12). Water pumped from the HSDP-1 well is

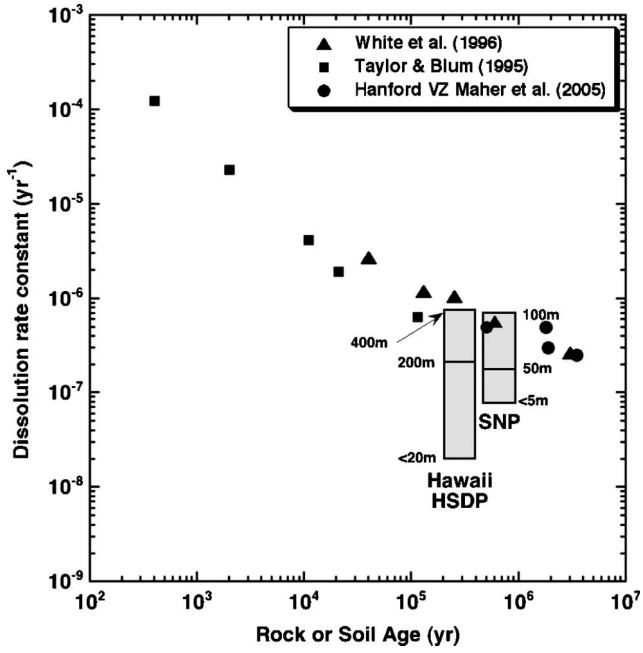

Fig. 12. Inferred solid phase bulk dissolution rate versus rock or soil age. Data shown are based on studies of soils (White et al., 1996; Taylor and Blum, 1995) and vadose zone unconsolidated sedimentary rocks (Maher et al., 2003). The base of the vertical bars shown for Hawaii–HSDP and the Snake River Plain aquifer (SNP) are the values of dissolution rate that would be inferred for these low-temperature fractured-rock aquifers with a standard porous flow model (Eq. (8)) and using the available Sr isotopic data (Thomas et al., 1996; Johnson et al., 2000). The vertical bars show the relationship between the inferred matrix dissolution rate (R_m) and the fracture spacing. For the Hawaii data, the inferred reaction rate is similar to that of the soils for an average fracture spacing of 300–400 m, and for the SNP, the fracture spacing would have to be 75–100 m to bring the estimated dissolution rate into the range for the granular materials.

observed to have $^{87}Sr/^{86}Sr$ that is significantly displaced from that of seawater in the direction of the basalt isotopic ratio (Thomas et al., 1996). Radiocarbon data are available from one sample of water for which there is also Sr isotopic data, and the raw radiocarbon age is about 7200 years. When the raw age is corrected for the apparent age of Pacific water at the likely depth of recharge, the net water age is about 5800 years. Since the Sr concentration of both the water and rocks is known quite well ($C_s/C_f = 42 \pm 4$), the dissolution rate of the basalt (or weathering rate) can be calculated for the porous flow model with the only unknown parameter being the porosity. Setting the spatial derivative to zero in Eq. (5a) and integrating yields

$$\frac{(r_s - r_f)}{(r_s - r_f)_0} = \exp\left[-\frac{(1-\phi_m)C_s\rho_s}{\phi_m C_f \rho_f} R t_R\right], \quad (46)$$

where t_R is the total amount of time the fluid reacts with the solid as it passes through the system and is taken to be the radiocarbon age of 5800 years. Solving for R in this equation yields

$$R_{sp} = \frac{-\phi_m C_f \rho_f}{(1-\phi_m)C_s\rho_s t_R} \ln\frac{(r_s - r_f)}{(r_s - r_f)_0}. \quad (47)$$

Substituting the appropriate values yields $R_{sp} = 1.1 \times 10^{-7}\ \phi_m/(1-\phi_m)$. Porosity in these rocks is in the range 0–20% for hand specimen sized samples (Moore, 2001). For a porosity of 0.1 ± 0.05 this yields for the dissolution rate $1.1(\pm 0.5) \times 10^{-8}\ yr^{-1}$. In Fig. 12, this result is compared to other estimates of natural mineral dissolution rates based on studies of soils (Taylor and Blum, 1995; White et al., 1996), and vadose zone pore fluids (Maher et al., 2003, 2006). As noted in these previous studies, there is an empirical relationship between dissolution rate and the age of the soil or sediment.

In Fig. 12, the HSDP data are plotted at an age of 200,000–400,000 years, the age of basalt lavas that compose the aquifer (Sharp et al., 1996). The inferred dissolution rate range is about 100 times smaller than those measured for other materials of the same age. The question is whether this discrepancy can be attributed to the effects of fracture flow. If the flow is confined to fractures, and if the fracture spacing is large compared to the diffusive reaction length of Sr for the system, then the apparent reaction rate will be smaller than the actual dissolution rate in the basalts. The value of L_{Sr} for $R_m = R_{sp} = 1.1 \times 10^{-8}\ yr^{-1}$ is about 30 m. Therefore for fracture spacing up to about 30 m, the inferred reaction rate for a fracture-flow system does not change significantly. To increase the reaction rate by a factor of 100 requires that $b = 20L_{sp}$, or 600 m (Eq. (33)). This distance is about 1/20 of the total distance the water is flowing and it is possible that the effective fracture spacing is this large. Fracture flow would also affect the interpretation of the radiocarbon age. However, with regard to the water age, for large fracture spacing the primary concern is the width of the "fracture" or high permeability zone relative to the decay length of ^{14}C (about 1 m; Eq. (44)). If the flow zone is 1–10-m thick, the water age is smaller than the radiocarbon age by a factor of 2.8–1.2. If the water age is, for example, half the radiocarbon age, and the fracture spacing is 300–400 m, the estimated dissolution rate for the basalts would be more in line with other estimates for rocks and soils of the same age. So it is plausible that the low dissolution rate calculated from Sr isotopes for the Hawaiian basalts is due to the effects of fracture flow on both the Sr and C isotopes.

The $^{87}Sr/^{86}Sr$ of dissolved Sr in the groundwater of the Snake River plain aquifer are observed to decrease systematically along the flow path and are interpreted as an effect of slow dissolution of the basalt (Johnson et al., 2000). For the typical values of dr_f/dx and the estimated flow velocity ($0.0003\ km^{-1}$ and $300\ m\ yr^{-1}$), Johnson et al. (2000) estimate a value of $R_{sp} = 5 \times 10^{-8}\ yr^{-1}$ ($C_s/C_f = 1500$, $\phi = 0.2$). The age of the basalts is between a few hundred thousand years and 1 million years (Fig. 12), so in this case as well the dissolution rate appears to be low relative to granular materials of the same age by a factor of about 10. The value of L_{Sr} calculated using R_{sp} is about 5 m. As shown in Fig. 12, the dissolution rate could be in the range of the granular materials for fracture spacing of 100 m, which is plausible fracture spacing for the Snake River Plain aquifer.

7.2. Fracture spacing in MOR hydrothermal systems

For mid-ocean ridge hydrothermal systems, cold seawater circulates down and through the basalt of the oceanic crust, is heated by and reacts with the hot rocks under the ridge, and returns to the surface where it is expelled back into the ocean. The isotopic composition of seawater is well known for both Sr ($^{87}Sr/^{86}Sr = 0.7092$) and oxygen ($\delta^{18}O = 0$). These values are uniform throughout the oceans (there are small variations of $\delta^{18}O$; Shanks et al., 1995), and represent the values in the fluids as they enter the reactive region of the hydrothermal system. The isotopic values for the basalt of the oceanic crust are also well known and relatively uniform ($^{87}Sr/^{86}Sr = 0.7025$ and $\delta^{18}O = +6$).

To apply the model to a MOR hydrothermal system, the diffusive reaction lengths for Sr and O isotopes are needed, which in turn requires values for fluid-phase diffusivities (D_i), as well as K_i, R, and ϕ. The matrix porosity used is based on the data of Alt (1995). The reaction rate is estimated in the following way. The available data (e.g., as shown in Fig. 13) suggest that O isotope ratios in the fluid phase shift by 20–60% of the way from the seawater value (0) to the value (+2.8) that corresponds to isotopic equilibrium with the host basalt at 350 °C. Based on the example shown in Fig. 4b, it is a reasonable first approximation to assume that the fractures are sufficiently closely spaced that the reaction rate inferred from O isotopes is close to that for a sp system. Setting the spatial derivative to zero in Eq. (5a) and integrating yields:

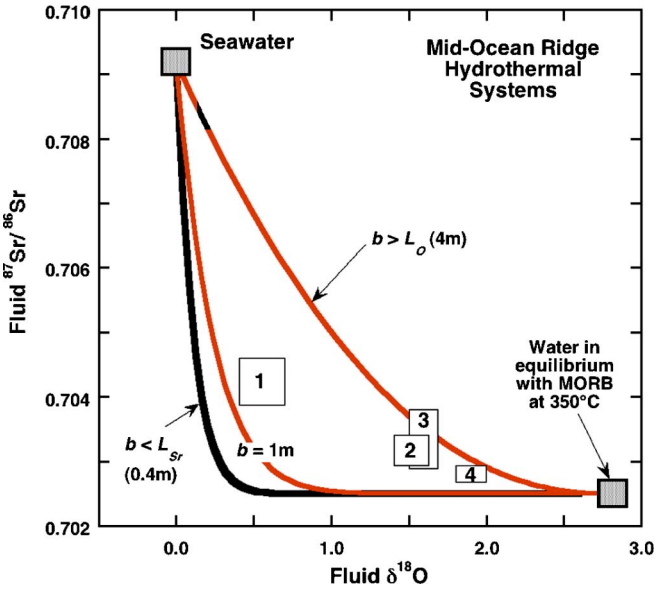

Fig. 13. Expected and observed relationship between $^{87}Sr/^{86}Sr$ and $\delta^{18}O$ values of hydrothermal fluids exiting mid-ocean ridge systems. The numbered squares correspond to data from different ocean ridge localities. 1: 11–13 °N East Pacific Rise (Campbell et al., 1994); Shanks et al., 1995; 2: OBS, 21 °N on the East Pacific Rise (Albarede et al., 1981; Campbell et al., 1988a; Shanks et al., 1995); 3: TAG hydrothermal mound, ODP Leg 158 (Gamo et al., 1996; Humphries et al., 1996; Teagle et al., 1998); 4: Mid Atlantic Ridge, MARK (Campbell et al., 1988b, 1994; Shanks et al., 1995). The data correspond to model fracture spacings, b, of about 1 m to greater than 4 m. Parameters used to calculate the curves (those not shown in the figure) are: $R = 0.0005\ yr^{-1}$, $D_O = 0.5\ m^2\ yr^{-1}$, $D_{Sr} = 0.1\ m^2\ yr^{-1}$, $\phi = 0.01$, $\rho_s/\rho_f = 2.5$, $K_{Sr} = 15$, and $K_O = 0.6$. The inferred fracture spacing is approximately proportional to $(D_i\phi/RK_i)^{1/2}$.

$$\frac{(r_s - \alpha r_f)}{(r_s - \alpha r_f)_0} = \frac{\delta_s - \delta_f(t) - \Delta}{\delta_s - \delta_f(0) - \Delta} = \exp\left[-\frac{(1-\phi_m)C_s\rho_s}{\phi_m C_f \rho_f} R t_R\right], \quad (48)$$

where t_R is the total amount of time the fluid reacts with the solid as it passes through the hydrothermal system. Substituting 0.8 to 0.4 for the ratio on the left side, and the values $\phi_m = 0.01$, $C_s/C_f = 0.6$ and $\rho_s/\rho_f = 2.5$, yields a range of values for Rt_R of 0.0006 to 0.0024. The evidence cited by Kadko and Moore (1988), and calculations of heat and mass transfer (Fisher et al., 2003) suggest that the time spent in the reaction zone is only about 3 years. If this result is used for t_R, then the deduced range of values for R is 2×10^{-4}–$8\times10^{-4}\ yr^{-1}$. For a matrix porosity of 0.01, a reaction rate of $5\times10^{-4}\ yr^{-1}$ ($R/\phi = 5\times10^{-2}\ yr^{-1}$), and $D_O = 0.5\ m^2\ yr^{-1}$, the reaction length for O isotopes is about 4 m for this system. For Sr, assuming $K_{Sr} = 15$ and $D_{Sr} = 0.1\ m^2\ yr^{-1}$, the corresponding reaction length is about 40 cm.

The data from mid-ocean ridge hydrothermal vents that do not show obvious sediment involvement (Fig. 13; references given in the figure caption) in most cases show shifts in $\delta^{18}O$ that are larger than expected relative to the shifts in $^{87}Sr/^{86}Sr$. The larger $\delta^{18}O$ shifts are consistent with the model predictions if the fracture spacing is larger than L_{Sr}. The contours on the figure show that the data suggest fracture spacings between about 1 m (about 3 times the value of L_{Sr}) and 4 m (the value of L_O).

The deduced fracture spacing for the MOR hydrothermal systems is plausible, but this calculation is meant more as an illustration of the application of the model than as a definitive conclusion. While there are a number of theoretical and observational constraints on the deep structure of MOR hydrothermal systems (e.g., Bickle and Teagle, 1992; Alt, 1995; Bickle et al., 1998; Fisher and Becker, 2000; Schultz and Elderfield, 1999), there is still uncertainty about the details. There are several potential problems that affect the interpretation of the data in Fig. 13. For example, the fluids traverse a range of temperatures while interacting with the rocks, which affects the calculated value of the $\delta^{18}O$ of equilibrated fluid and hence the location of the L/b contours. The reaction rate and matrix porosity are not well known. However, the deduced fracture spacing scales approximately with $(\phi/R)^{1/2}$, so uncertainties of a factor of 4 in this ratio change the inferred spacing only by a factor of 2. The fact that the fluid isotopic compositions fit the model reasonably well is encouraging, and somewhat surprising, considering the possible complications. The discrepancy between the shifts in $\delta^{18}O$ for the solid phase (in ophiolites), in comparison to $^{87}Sr/^{86}Sr$, has been previously noted (e.g., Bickle and Teagle, 1992), and is complementary to the matrix diffusion effects on the fluids. Bickle et al. (1998) did not find evidence of sharp Sr isotope gradients near inferred fracture zones in the Troodos ophiolite, but did observe gradients, as well as a large amount of variability in the measured $^{87}Sr/^{86}Sr$ values of whole rocks and minerals. The Bickle et al. (1998) observations are reasonably consistent with the predictions made here. For fracture spacings of ca. 1–2 m (about 2.5–5 times L_{Sr}), there would not necessarily by sharp gradients of $^{87}Sr/^{86}Sr$ near fractures (Fig. 4b), and furthermore, because fluid flow may continually shift to new fractures during the protracted lifetime of a hydrothermal system, the resultant spatial patterns can be complicated. Deducing the properties of fossil hydrothermal systems from rock properties measured long after the ocean floor has moved away from the ridge is in many ways more difficult than the approach presented here, because the rocks integrate over the entire active history of the hydrothermal system.

8. Discussion

The model described here allows the effects of matrix diffusion in fractured rock–fluid systems to be evaluated using isotopic data. The magnitude of the matrix diffusion effects can be calculated from the ratio of the diffusive reaction length (L) to the fracture spacing. The reaction length varies among elements with naturally occurring isotopic variations. The primary observable effect attributable to matrix diffusion is that elements with smaller L values ap-

pear to react more slowly with the host rocks than elements with larger L values. The difference in apparent reactivity between two elements is detectable only if the fracture spacing is significantly larger than the L value of at least one of the elements. If the L values can be estimated, then the fracture spacing can be inferred. In systems where the fractures are more closely spaced than the smallest L value, a sp formulation will adequately describe the isotopic evolution of moving fracture fluids. The model therefore provides a means of evaluating the need for a dp formulation for describing isotopic data from fluids.

There are several potential applications of the matrix diffusion effects in isotopic systems. In geothermal systems, isotopic data could be used to infer fracture spacing as in the example described for mid-ocean ridges. The information derived may be unique in that the inferred spacing applies to the fractures actually carrying the bulk of the fluid. Once this fracture spacing is known, it allows estimation of the thermal response time of the reservoir to perturbations in flow or to the temperature of injected fluids. In groundwater systems, information on fracture spacing and L values for some elements can be used to infer the behavior of other elements. For example, retardation effects in fractured rocks are highly dependent on the accessibility of the matrix to chemical interaction with the fracture fluids. This accessibility is reflected by the reaction length parameter. If the matrix diffusion effects can be detected for an element with variable isotopic ratios, it is then generally possible to calculate the matrix diffusion effects for other elements based on their concentrations in the fluids (their K_i values). Hence the dp model, coupled with appropriate field geochemical data, could help in understanding the transport of radionuclides and other groundwater contaminants in fractured rock systems.

The interpretation of isotopic data from fluid–rock systems must account for matrix diffusion effects. The inferred amount of reaction for one isotope system is typically used to infer the amount of reaction for another isotope. For example, if Sr isotopes in groundwater suggest that only a few percent reaction with host rocks occurs along a flow path, this information is typically used to infer that no detectable oxygen isotope shift can result from reaction. Hence any observed differences in $\delta^{18}O$ along the flow path are attributed to another process (such as admixing of water from a different source). The dp model suggests that such inferences may be incorrect in some cases. In groundwater systems, the value of L_{Sr} is typically 50–100 times smaller than the value of L_O. Consequently, the Sr isotope shifts can underestimate the corresponding O isotope shifts by a large factor.

The applicability of the model presented depends to a significant degree on the magnitude of natural bulk reaction rates, which are represented in the model by the parameters R, R_{sp}, and R_m. In natural systems, empirical evidence suggests that the range of values is from about 10^{-4} to about 10^{-9} yr^{-1} in groundwater, geothermal, metamorphic and diagenetic settings (Richter and Liang, 1993; Taylor and Blum, 1995; White et al., 1996; Johnson et al., 2000; Baxter and DePaolo, 2000; Maher et al., 2004). Slow reaction rates tend to ensure that the condition expressed in Eq. (7) ($MK \gg \tau_a/\tau_f$) and the condition $\tau_a/\tau_f \leqslant 1$ are likely to be common. The reaction rates predicted by laboratory studies, applied to natural systems through transition state theory or some variant thereof, would suggest that reaction rates are much faster (order 100–10^{-2} yr^{-1}) (e.g., Walther and Wood, 1986; Walther, 1994; Maher et al., 2006), which would predict that the above conditions are not generally met. Most modeling that has been done of reactive transport in fractured media (e.g., Bickle and McKenzie, 1987; Bickle, 1992; Steefel and Lichtner, 1998a,b) assumed or calculated fast reaction rates and hence deal with effects that represent quite different conditions than those assumed for the purpose of this work. The available data strongly suggest that the reaction rates discussed in this work are relevant and typical of most natural fluid–rock systems, although not necessarily to solutions of extreme composition as treated by Steefel and Lichtner (1998b).

9. Conclusions

A model has been developed that describes the effects of matrix diffusion on isotopic exchange between fluids and rocks in geo-hydrological systems. The model is not completely general, but results in a simple relationship that allows the effects of matrix diffusion on the isotopes of a particular element to be estimated based on the ratio of the diffusive reaction length (L) to the fracture spacing. The diffusive reaction length for a given chemical element depends on the dissolution and precipitation rates affecting the solid matrix, the concentration of the element in the solid and the fluid, the porosity, and the aqueous diffusivity. When used with data from two or more isotopic systems, it may be possible to use the model to estimate fracture spacing in natural systems from the isotopic characteristics of rocks and fluids. The advantage of this approach is that it gives an estimate of the spacing of the fluid-carrying fractures, which is difficult to obtain otherwise.

An example of an application to hydrothermal systems is given using Sr and O isotopic data from mid-ocean ridge hydrothermal vent fluids. The data suggest that fracture spacing is 1–4 m in these systems, although the precise value of the inferred fracture spacing is subject to uncertainties in some of the input parameters. Application of the model to groundwater hosted in fractured basalt suggests that fracture–matrix effects cause groundwater Sr isotope ratios to underestimate the basalt dissolution rates. In general, the dp model presented here may help in the interpretation of isotopic data from fractured rock systems. A particularly useful aspect of the model is that it provides a straightforward way to establish the necessity of treating isotopic data on fluid–rock systems with a dp model as opposed to a sp model. The model also allows one to estimate

the effect that matrix diffusion will have on isotopic exchange rates for a given fracture spacing.

Acknowledgments

This research was supported by the Director, Office of Energy Research, Basic Energy Sciences, Chemical Sciences Division of the US Department of Energy under Contract No. DE-AC02-05CH11231. The manuscript benefited from comments by F.M. Richter, B.M. Kennedy, C.F. Steefel, and N. Spycher, and reviews by A.T. Fisher, M.J. Bickle and two anonymous reviewers. Completion of the research was aided by a Fellowship from the John Simon Guggenheim Foundation.

Associate editor: Chen Zhu

References

Albarede, F., Michard, A., Minster, J.F., Michard, G., 1981. $^{87}Sr/^{86}Sr$ ratios in hydrothermal waters and deposits from the East Pacific Rise at 21 degrees N. *Earth Planet. Sci. Lett.* **55**, 229–236.

Alt, J.C., 1995. Subseafloor processes in mid-ocean ridge hydrothermal systems. In: Humphries, S.E., Zierenberg, R.A., Mullineaux, L.S., Thomson, R.E. (Eds.), Seafloor Hydrothermal Systems. American Geophysical Union Monograph 91, pp. 85–114.

Baxter, E., DePaolo, D.J., 2000. Field evidence for slow metamorphic reaction rates at 500–600 °C. *Science* **288**, 1411–1414.

Bear, J., 1979. *Dynamics of Fluids in Porous Media*. Elsevier, New York.

Bear, J., 1992. Modeling flow and contaminant transport in fractured rocks. In: Bear, J., Tsang, C.-F., de Marsily, G. (Eds.), *Flow and Contaminant Transport in Fractured Rock*. Academic Press, pp. 1–37.

Bickle, M.J., 1992. Transport mechanisms by fluid-flow in metamorphic rocks: Oxygen and strontium decoupling in the Trois Seigneurs Massif—A consequence of kinetic dispersion? *Am. J. Sci.* **292**, 289–316.

Bickle, M.J., Chapman, H.J., 1990. Strontium and oxygen isotope decoupling in the Hercynian Trois Seigneurs Massif, Pyrenees: evidence for fluid circulation in a brittle regime. *Contrib. Mineral. Petrol.* **104**, 332–347.

Bickle, M.J., McKenzie, D., 1987. The transport of heat and matter by fluids during metamorphism. *Contrib. Mineral. Petrol.* **95**, 384–392.

Bickle, M.J., Teagle, D.A.H., 1992. Strontium alteration in the Troodos Ophiolite; implications for fluid fluxes and geochemical transport in mid-ocean ridge hydrothermal systems. *Earth Planet. Sci. Lett.* **113**, 219–237.

Bickle, M.J., Teagle, D.A.H., Beynon, J., Chapman, H.J., 1998. The structure and controls on fluid–rock interactions in ocean ridge hydrothermal systems: constraints from the Troodos ophiolite. *Special Publ. Geol. Soc. London* **148**, 127–152.

Blattner, P., Lassey, K.R., 1989. Stable isotope exchange fronts, Damkohler numbers, and fluid–rock ratios. *Chem. Geol.* **78**, 381–392.

Campbell, A.C., Bowers, T.S., Measures, C.I., Falkner, K.K., Khadem, M., Edmond, J.M., 1988a. A time-series of vent fluid compositions from 21 °N East Pacific Rise (1979, 1981, 1985) and the Guaymas Basin, Gulf of California (1982, 1985). *J. Geophys. Res.* **93**, 4537–4549.

Campbell, A.C., Palmer, M.R., Klinkhammer, G.P., Bowers, T.S., Edmond, J.M., Lawrence, J.R., Casey, J.F., Humphris, S., Rona, P., Karson, J.A., 1988b. Chemistry of hot springs on the Mid-Atlantic Ridge. *Nature* **335**, 514–519.

Campbell, A.C., German, C., Palmer, M.R., Edmond, J.M., 1994. Chemistry of hydrothermal fluids from the Escanaba Trough, Gorda Ridge. In: Morton, J.L., Zierenberg, R.A., Reiss, C.A (Eds.), Geologic, Hydrothermal, and Biologic Studies at Escanaba Trough, Offshore Northern California. US Geological Survey Bulletin 2022, pp. 201–221.

Criss, R.E., Gregory, R.T., Taylor, H.P., 1987. Kinetic theory of oxygen isotopic exchange between minerals and water. *Geochim. Cosmochim. Acta* **51**, 1099–1108.

Criss, R.E., 1999. *Principles of Stable Isotope Distribution*. Oxford University Press, New York.

DePaolo, D.J., Getty, S.R., 1996. Models of isotopic exchange in reactive fluid–rock systems: Implications for geochronology in metamorphic rocks. *Geochim. Cosmochim. Acta* **60**, 3933–3947.

Evans, D.D., Nicholson, T.J., 1987. Flow and transport through unsaturated fractured rock: An overview. In: Evans, D.D., Nicholson, T.J. (Eds.), Flow and Transport Through Unsaturated Fractured Rock. American Geophysical Union Monograph 42, pp. 1–10.

Fisher, A.T., Becker, K., 2000. Channelized fluid flow in oceanic crust reconciles heat-flow and permeability data. *Nature* **403**, 71–74.

Fisher, A.T., Davis, E.E., Hutnak, M., Spiess, V., Zuhlsdorff, L., Cherkaoui, A., Christiansen, L., Edwards, K., Macdona, L.R., Villinger, H., Mottl, M.J., Wheat, C.G., Becker, K., 2003. Hydrothermal recharge and discharge across 50 km guided by seamounts on a young ridge flank. *Nature* **421**, 618–621.

Gamo, T., Chiba, H., Masuda, H., Edmonds, H.N., Fujioka, K., Kodama, Y., Nanba, H., Sano, Y., Rona, P.A., Von Herzen, R.P., 1996. Chemical characteristics of hydrothermal fluids from the TAG mound of the Mid-Atlantic Ridge in August 1994; implications for spatial and temporal variability of hydrothermal activity. *Geophys. Res. Lett.* **23**, 3483–3486.

Gregory, R.T., Criss, R.E., Taylor, H.P., 1989. Oxygen isotope exchange kinetics of mineral pairs in closed and open systems—applications to problems of hydrothermal alteration of igneous rocks and precambrian iron formations. *Chem. Geol.* **75**, 1–42.

Humphries, S.E., Herzig, P.M., Miller, D.J., et al., 1996. Proceedings of ODP. Initial Reports 158, College Station, Texas, 384 pp.

Johnson, T.M., DePaolo, D.J., 1994. Interpretation of isotopic data in groundwater–rock systems: model development and application to Sr isotopic data from Yucca Mountain. *Water Resources Res.* **30**, 1571–1587.

Johnson, T.M., DePaolo, D.J., 1997a. Rapid exchange effects on isotope ratios in groundwater. 1. Development of a transport–dissolution-exchange model. *Water Resources Res.* **33**, 187–195.

Johnson, T.M., DePaolo, D.J., 1997b. Rapid exchange effects on isotope ratios in groundwater systems. 2. Flow investigation using Sr isotope ratios. *Water Resources Res.* **33**, 197–205.

Johnson, T.M., Roback, R.C., McLing, T.L., Bullen, T.D., DePaolo, D.J., Doughty, C., Hunt, R.J., Smith, R.W., Cecil, L.D., Murrell, M.T., 2000. Groundwater "fast paths" in the Snake River Plain aquifer: Radiogenic isotope ratios as natural groundwater tracers. *Geology* **28**, 871–874.

Kadko, D., Moore, W., 1988. Radiochemical constraints on the crustal residence time of submarine hydrothermal fluids: Endeavor Ridge. *Geochim. Cosmochim. Acta* **52**, 659–668.

Lasaga, A.C., 1984. Chemical kinetics of water–rock interaction. *J. Geophys. Res.* **89**, 4009–4025.

Lasaga, A.C., Rye, D.M., 1993. Fluid flow and chemical reaction kinetics in metamorphic systems. *Am. J. Sci.* **293**, 361–404.

Lassey, K.R., Blattner, P., 1988. Kinetically controlled oxygen isotope exchange between fluid and rock in one dimensional advective flow. *Geochim. Cosmochim. Acta* **52**, 2169–2175.

Magaritz, M., Taylor, H.P., 1976. Isotopic evidence for meteoric hydrothermal alteration of plutonic igneous rocks in Yakutat Bay and Skagway areas, Alaska. *Earth Planet. Sci. Lett.* **30**, 179–190.

Maher, K., DePaolo, D.J., Conrad, M.S., Serne, R.J., 2003. Vadose zone infiltration rate at Hanford, Washington, inferred from Sr isotope measurements. *Water Resources Res.* **39** (8), 1204–1217.

Maher, K., DePaolo, D.J., Lin, J.C.-F., 2004. Rates of diagenetic reactions in deep-sea sediment: In situ measurement using $^{234}U/^{238}U$ of pore fluids. *Geochim. Cosmochim. Acta* **68**, 4629–4648.

Maher, K., Steefel, C.I., DePaolo, D.J., Viani, B.E., 2006. The mineral dissolution rate conundrum: Insights from reactive transport modeling of U isotopes and pore fluid chemistry in marine sediments. *Geochim. Cosmochim. Acta* **70**, 337–363.

Maloszewski, P., Zuber, A., 1991. Influence of matrix diffusion and exchange reactions on radiocarbon ages in fissured carbonate aquifers. *Water Resources Res.* **27**, 1937–1945.

Moore, J.G., 2001. Density of basalt core from Hilo drill hole, Hawaii. *J. Volcanol. Geotherm. Res.* **112**, 221–230.

Navon, O., Stolper, E., 1987. Geochemical consequences of melt percolation: the upper mantle as a chromatographic column. *J. Geol.* **95**, 285–307.

Neretneiks, I., 1992. Solute transport in fractured rock—applications to radionuclide waste repositories. In: Tsang, C.-F., de Marsily, G. (Eds.), *Flow and Contaminant Transport in Fractured Rock*. Academic Press, pp. 39–128.

Richter, F.M., DePaolo, D.J., 1987. Numerical models for diagenesis and the Neogene Sr isotopic evolution of seawater from DSDP Site 590B. *Earth Planet. Sci. Let.* **83**, 27–38.

Richter, F.M., DePaolo, D.J., 1988. Diagenesis and Sr isotopic evolution of seawater using data from DSDP 590B and 575. *Earth Planet. Sci. Lett.* **90**, 382–394.

Richter, F.M., Liang, Y., 1993. The rate and consequences of Sr diagenesis in deep-sea carbonates. *Earth Planet. Sci. Lett.* **117**, 553–565.

Sanford, W., 1997. Correcting for diffusion in Carbon-14 dating of groundwater. *Ground Water* **35**, 357–361.

Schrag, D.P., DePaolo, D.J., Richter, F.M., 1992. Oxygen isotope exchange in a two-layer model of oceanic crust. *Earth Planet. Sci. Lett.* **111**, 305–317.

Schrag, D.P., DePaolo, D.J., Richter, F.M., 1995. Reconstructing past sea surface temperatures—correcting for diagenesis of bulk marine carbonate. *Geochim. Cosmochim. Acta* **59**, 2265–2278.

Schultz, A., Elderfield, H., 1999. Controls on the physics and chemistry of seafloor hydrothermal systems. In: Cann, J.R., Elderfield, H., Laughton, A. (Eds.), *Mid-Ocean Ridges: Dynamics of processes associated with creation of new ocean crust*. Cambridge University Press, pp. 171–209.

Shanks, W.C. III, Bohlke, J.K., Seal, R.R. II, 1995. Stable isotopes in mid-ocean ridge hydrothermal systems: Interactions between fluids, minerals, and organisms. In: Humphries, S.E., Zierenberg, R.A., Mullineaux, L.S., Thomson, R.E. (Eds.), Seafloor Hydrothermal Systems. American Geophysical Union Monograph 91, pp. 194–221.

Sharp, W.D., Turrin, B.D., Renne, P.R., Lanphere, M.A., 1996. $^{40}Ar/^{39}Ar$ and K/Ar dating of lavas from the Hilo 1-km core hole, Hawaii Scientific Drilling Project. *J. Geophys. Res.* **101** (5), 607–611, 616..

Skelton, A.D.L., Bickle, M.J., Graham, C.M., 1997. Fluid-flux and reaction rate from advective-diffusive carbonation of mafic sill margins in the Dalradian, southwest Scottish Highlands. *Earth Planet. Sci. Lett.* **146**, 527–539.

Steefel, C.I., Lichtner, P.C., 1998a. Multicomponent reactive transport in discrete fractures: I. Controls on reaction front geometry. *J. Hydrol.* **209**, 186–199.

Steefel, C.I., Lichtner, P.C., 1998b. Multicomponent reactive transport in discrete fractures: II. Infiltration of hyperalkaline groundwater at Maqarin, Jordan, a natural analogue site. *J. Hydrol.* **209**, 200–224.

Sudicky, E.A., Frind, E.O., 1982. Contaminant transport in fractured porous media: Analytical solutions for a system of parallel fractures. *Water Resources Res.* **18**, 1634–1642.

Tang, D.H., Frind, E.O., Sudicky, E.A., 1981. Contaminant transport in fractured porous media: Analytical solution for a single fracture. *Water Resources Res.* **17**, 555–564.

Taylor, H.P., 1974. The application of oxygen and hydrogen isotope studies to problems of hydrothermal alteration and ore deposition. *Econ. Geol.* **69**, 843–883.

Taylor, A., Blum, J.D., 1995. Relation between soil age and silicate weathering rates determined from the chemical evolution of a glacial chronosequence. *Geology* **23**, 979–982.

Teagle, D.A.H., Alt, J.C., Chiba, H., Humphris, S.E., Halliday, A.N., 1998. Strontium and oxygen isotopic constraints on fluid mixing, alteration and mineralization in the TAG hydrothermal deposit. *Chem. Geol.* **149**, 1–24.

Thomas, D.M., Paillet, F.L., Conrad, M.E., 1996. Hydrogeology of the Hawaii Scientific Drilling Project borehole KP-1; 2, Groundwater geochemistry and regional flow patterns. *J. Geophys. Res.* **101**, 11683–11694.

Walther, J.V., Wood, B.J., 1986. Mineral fluid reaction rates. In: Walther, J.V., Wood, B.J. (Eds.), *Fluid–Rock Interactions during Metamorphism*. Springer-Verlag, New York, pp. 194–212.

Walther, J.V., 1994. Fluid–rock reactions during metamorphism at mid-crustal conditions. *J. Geol.* **102**, 559–570.

White, A.F., Blum, A.E., Schulz, M.S., Bullen, T.D., Harden, J.W., Peterson, M.L., 1996. Chemical weathering rates of a soil chronosequence on granitic alluvium: I. Quantification of mineralogical and surface area changes and calculation of primary silicate reaction rates. *Geochim. Cosmochim. Acta* **60**, 2533–2550.

Wilson, M.L., Dudley, A.L., 1987. Radionuclide transport in an unsaturated, fractured medium. In: Evans, D.D., Nicholson, T.J. (Eds.), Flow and Transport Through Unsaturated Fractured Rock. American Geophysical Union Monograph 42, pp. 23–29.